

Elucidating ATP's Role as Solubilizer of Biomolecular Aggregate

Reviewed Preprint

v2 • September 24, 2024

Revised by authors

Reviewed Preprint

v1 • July 10, 2024

Susmita Sarkar, Saurabh Gupta, Chiranjit Mahato, Dibyendu Das, Jagannath Mondal 

Tata Institute of Fundamental Research Hyderabad, Telangana, India, 500046 • Indian Institute of Science Education and Research, Kolkata, Campus Rd, Mohanpur, Haringhata Farm, West Bengal 741246

 https://en.wikipedia.org/wiki/Open_access
 Copyright information

Abstract

Proteins occurring in significantly high concentrations in cellular environments (over 100 mg/mL) and functioning in crowded cytoplasm, often face the prodigious challenges of aggregation which are the pathological hallmark of aging and are critically responsible for a wide spectrum of rising human diseases. Here we combine a joint-venture of complementary wet-lab experiment and molecular simulation to discern the potential ability of adenosine triphosphate (ATP) as solubilizer of protein aggregates. We show that ATP prevents both condensation of aggregation-prone intrinsically disordered protein A β 40 and promotes dissolution of pre-formed aggregates. Computer simulation links ATP's solubilizing role to its ability to modulate protein's structural plasticity by unwinding protein conformation. We show that ATP is positioned as a superior biological solubilizer of protein aggregates over traditional chemical hydrotropes, potentially holding promises in therapeutic interventions in protein-aggregation related diseases. Going beyond its conventional activity as energy currency, the amphiphilic nature of ATP enables its protein-specific interaction that would enhance ATP's efficiency in cellular processes.

eLife assessment

The authors combined molecular dynamics simulations and experiments to study the role of ATP as a hydrotrope of protein aggregates. The topic is of major current interest and thus the study potentially makes an **important** contribution to the community. With the revised version, the level of evidence is considered generally **solid**, although there remains concern regarding the unusually high ATP concentration used in the simulation.

<https://doi.org/10.7554/eLife.99150.2.sa3>

Introduction

Adenosine triphosphate (ATP), universally present in all living organisms, is recognized as a fundamental energy currency essential for a myriad of cellular processes. While its traditional role in energy metabolism is well-established, recent investigations have unveiled novel dimensions of ATP's involvement, specifically in protein stabilization and solubilization. Although

the canonical functions of ATP are comprehensively understood, its impact on cellular protein homeostasis, particularly in the prevention of aggregation and the maintenance of membraneless organelles, remains a subject of growing interest ^{1–4}.

Beyond its well-known chemical actions originating from high-energy phosphate bond breaking or allosteric effects during enzymatic catalysis, ATP exhibits contrasting physical biological roles, including the stabilization of soluble proteins ^{2,5,6} and the solubilization of insoluble proteins ^{1,2,7,10}. Proteome-wide profiling analyses emphasize ATP-mediated protein stabilization as a prevalent trait within the ensemble of proteins featuring an ATP recognition site ². Subsequent independent studies further validate ATP-mediated enhancement of protein stability for specific proteins, such as ubiquitin, malate dehydrogenase ⁵, and the TDP-43 RRM domain ⁶, all possessing an ATP-binding motif. Intriguingly, these proteins, where ATP functions as a substrate or allosteric modulator, typically require a low concentration of ATP (approximately 500 μ M) for its effects ².

Notably, the cellular cytoplasm maintains a significantly higher concentration of ATP (\sim 5mM), prompting questions about potential additional purpose for this elevated cytoplasmic ATP concentration beyond its conventional roles as an energy source and in protein stabilization, both typically requiring micromolar concentrations of ATP. As a potential function of the excess ATP concentration within the cell, a substantial influence on cellular protein homeostasis is observed, particularly in preventing protein aggregation ^{1,7,9,11–13} and maintaining the integrity of membraneless organelles (at a millimolar range of ATP concentration). ATP has demonstrated its capability to prevent the formation of protein aggregates, dissolve liquid-liquid phase-separated (LLPS) droplets, and disrupt pathogenic amyloid fibers ¹.

Investigations into ATP's impact on protein solubility and aggregation encompass a diverse array of proteins, including phase-separating proteins like FUS, TAF15, hnRNP A3, and PGL-3 ¹, as well as the aggregates of *Xenopus* oocyte nucleoli ¹¹. Elevated ATP concentrations are also observed in metabolically quiescent organs, such as the eye lens, where they prevent the crowding of γ -Crystallin ⁷. Proteome-wide profiling analyses underscore ATP's ability to manage the solubility of numerous proteins, indicating a broad impact on cellular protein solubility and aggregation propensity ².

Remarkably, a majority of proteins lacking any ATP-binding motif, are reported to undergo solubilization in the presence of ATP. Despite past conformational analyses of water-soluble ATP-binding proteins in the presence of ATP ², the role of ATP in biomolecular solubilization, specifically how ATP influences the structural plasticity of insoluble, non-ATP binding proteins, has yet to receive mainstream attention. In this investigation, we employ a combination of computer simulations and experimental techniques to explore how ATP influences the conformational behavior of two proteins situated at opposite ends of the structural spectrum of non-ATP binding proteins: the folded globular mini-protein Trp-cage and the amyloidogenic intrinsically disordered protein (IDP) A β 40, associated with Alzheimer's disease (**Figure 1**). Our study, incorporating ThT assay and Transmission Electron Microscopy, validates hypotheses generated through computer simulations regarding ATP's impact on the nucleating core of the A β 40 peptide segment. The results establish a clear correlation between ATP's effect on the conformational landscape of these proteins and its ability to impede the aggregation process, affirming its role as a solubilizing agent.

Results and Discussion

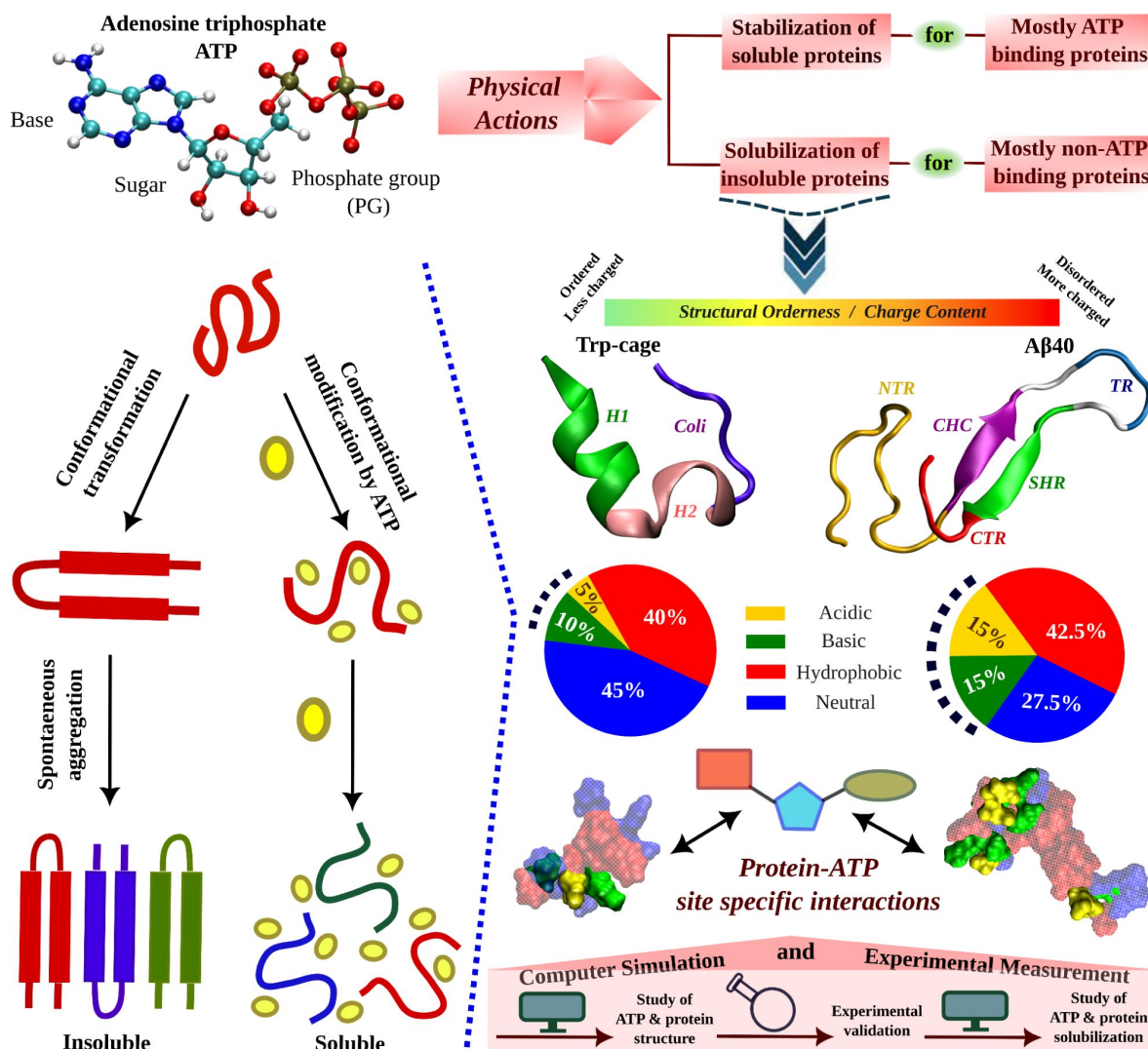


Figure 1

A schematic representation shows protein undergoes spontaneous aggregation in aqueous medium through specific conformational transformation prone to aggregation. ATP can prevent protein aggregation and improves its solubility. ATP's effect in protein conformational plasticity has been tested for two contrasting protein molecules belonging from two extreme spectrums of the protein family. One is the globular, structurally ordered protein Trp-cage and the other one is intrinsically disordered protein (IDP), Aβ40, containing comparatively more charged residues (according to the nature of typical IDPs). The highly aggregation prone Aβ40 protein is popularly well known for causing neurodegenerative disorders (*Alzheimer's disease, AD*). The structures of both the proteins are shown in the new cartoon representation highlighting the protein region wise coloration scheme. For Trp-cage the three distinct regions, 1. Helix (H1, 1-9), 2. 3-10 Helix (H2, 10-15) and 3. Coil (coil, 16-20) are shown in green, pink and navy blue colors respectively. For Aβ40, the 1. N-terminal region (NTR, 1-16), 2. central hydrophobic core (CHC, 17-21), 3. turn (TR, 24-27), 4. secondary hydrophobic region (SHR, 30-35), and the 5. C-terminal regions (CTR, 36-40) are shown in gold, purple, blue, green and red colors respectively. The hydrophobicity index of each of the proteins is shown in pie chart representation containing acidic (gold), basic (green), hydrophobic (red) and neutral (blue) residue content. Each of the proteins shown in the surface model are colored according to the respective hydrophobicity nature. Protein-ATP (base part: red, sugar moiety: cyan and phosphate group: green) site specific interactions are tested. The current study of ATP's effect on protein conformational plasticity is performed combining both simulation and experiment based on computational predictions validated by experimental measurement followed by computational reasoning and correlation of ATP driven conformational modification to protein aggregation scenario.

ATP's impact on a globular mini-protein

We initiated our investigation via computationally simulating ATP's effect on the archetypal monomeric form of mini-protein Trp-cage which is known to have a well-defined fold under native conditions (see [Figure 1](#)). The effects of ATP on the structure of the Trp-cage protein were investigated using classical molecular dynamics (MD) simulations. The protein was modeled with a99SB-*disp* forcefield and solvated with TIP4P-*disp* water molecules. The system was neutralized with chloride ions. The protein was simulated in aqueous solution and also in presence of ATP, at a temperature of 303 K. The precedent studies reporting the effect of ATP on structured proteins, had been performed by maintaining ATP:protein stoichiometric ratio in the range of 0.01×10^3 to 0.03×10^3 . Likewise, in our simulation with Trp-cage, the ATP:protein ratio of 0.02×10^3 was maintained. In this study, we opted to maintain the ATP stoichiometry consistent with biological conditions and previous in vitro experiments¹. Instead of keeping the protein concentration within the micromolar range and ATP concentration at the millimolar level, we chose this approach to avoid the need for an extremely large simulation box, which would greatly reduce computational efficiency by more than 150-fold.

Simulations were performed at three different concentrations of ATP.Mg⁺², 0 M (aqueous media), 0.1 M, and 0.5 M. For ensuring exhaustive exploration of protein conformational landscape condition, each condition was extensively simulated via replica exchange MD simulation (see method). The results showed that ATP caused the Trp-cage protein to unfold. This was evident from an increase in the protein's radius of gyration (R_g) and a decrease in the number of intra-chain contacts (see [Figure 2 A-C](#)). The R_g of the protein monotonically increased by the action of ATP compared to that of the neat water system in a concentration dependent manner ([Figure 2A](#)). The number of overall intra-chain contacts ([Figure 2B](#)) and native sub-set of intra-chain contacts ([Figure 2C](#)) monotonically decreased upon increasing the concentration of ATP from 0.1 M to 0.5 M. This is also evident from the inter-residue contact-map (see [Figure S1 A-B](#)). The two-dimensional free energy landscape of the Trp-cage protein was also calculated (see [Figure 2 D-F](#)). Since multiple previous studies has reported benchmarking of several features of proteins as well as IDPs using both linear and artificial neural network based dimension reduction techniques and have demonstrated that R_g , in combination with fraction of native contact serves as optimum features, we have chosen these two metrics for developing the 2D free energy profile^{14,15}. The landscape showed that the protein prefers to remain in its folded form (with less R_g and high native contacts) in the absence of ATP. However, in the presence of ATP, the landscape becomes more populated with conformations that have a higher R_g and fewer intra-chain contacts. This suggests that ATP drives the unfolding of the Trp-cage protein by stabilizing conformations that are more extended and disordered. The observation remains robust over the choice of force field. Similar to the results obtained with a99SB-*disp* forcefield, when the similar simulations were performed with Charmm36 force parameters of protein (with Charmm TIP3P water model) in 0 M and 0.5 M of ATP (modeled with Charmm36 force field parameters), the extension of the protein chain has been noted, as was characterized by the stabilization of protein conformations with higher R_g and lower native contacts is attained in presence of ATP ([figure S2](#)). The event of unfolding of the protein upon addition of ATP is also evident from the simulation snapshots (see [Figure G-H](#)). A comparative molecular analysis of secondary structure of Trp-cage in neat water versus ATP indicates reduction of both alpha-helical and 3-10 helical content ([figure 3 A-B](#)) along with inter-residue hydrogen bond ([figure S3](#)). Interestingly, the protein's solvent accessible surface area (SASA) increases slightly in presence of ATP ([figure 3 C](#)), implying that ATP can increase the solubility of protein, a point that we would later come back to.

The solvation shell of ATP around Trp-cage suggested its direct interaction with the protein (see [Figure 3 D](#) for a snapshot). Analysis of the preferential interaction coefficient (Γ) profiles (see method for definition) provided insights into the relative influence of different chemical components of ATP (triphosphate group, sugar moiety, and aromatic base) on the protein (see [Figure 3 E](#)). Consistently higher preferential interaction coefficient (Γ) profile of the aromatic

Protein: Trp-cage

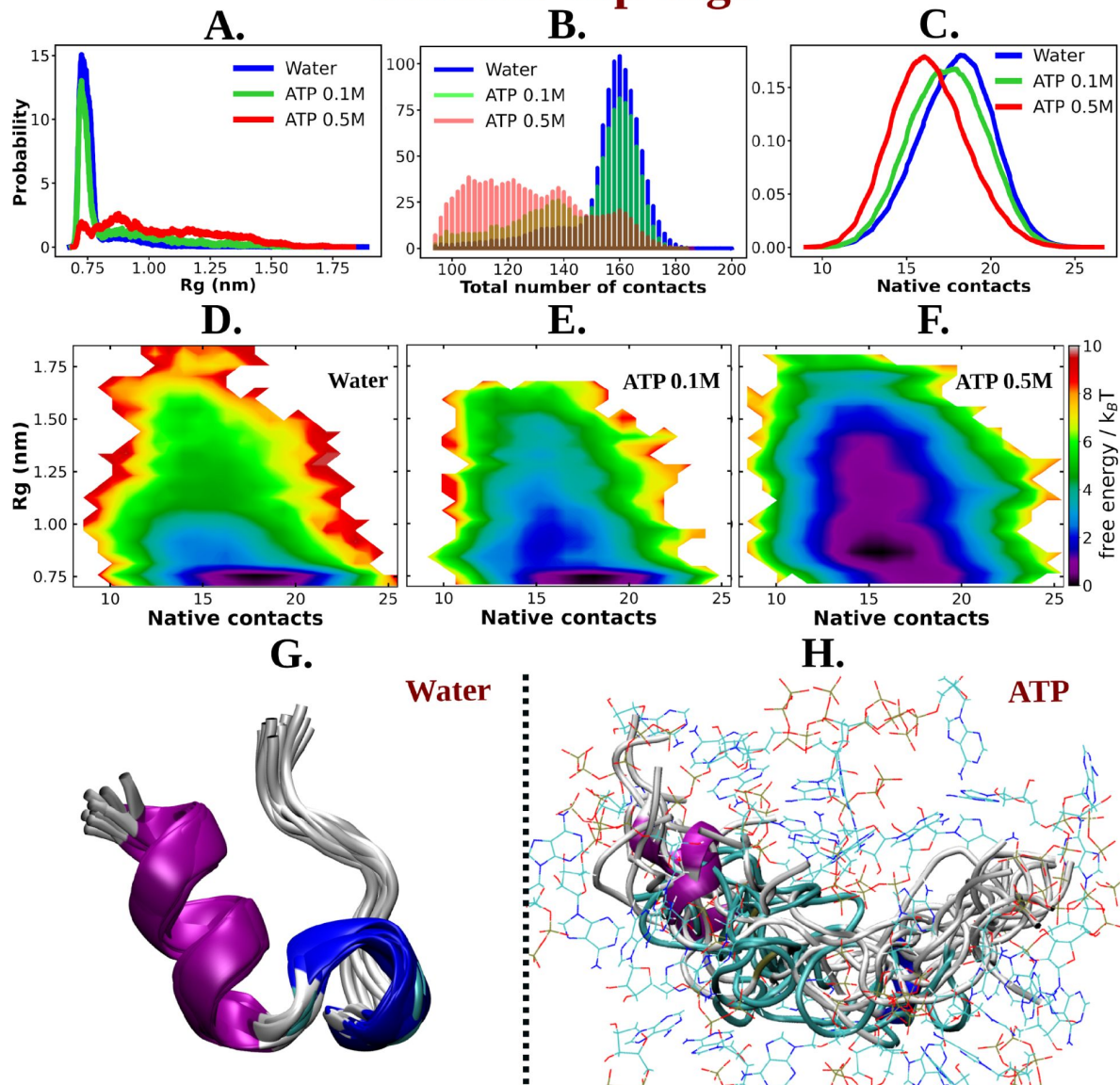


Figure 2

A. The probability distribution of R_g of Trp-cage compared in neat water and in 0.1 and 0.5 M ATP. B. Probability of the total number of contact formation among the residues of Trp-cage monomer are compared in absence (water) and presence of ATP (at 0.1 and 0.5 M). The probability distribution of native contacts (nc) of the protein in water and in 0.1 and 0.5 M ATP solutions are being shown in figure C. Figure D, E and F represent the 2D free energy profile of Trp-cage corresponding to the R_g and nc of the protein in water, 0.1 and 0.5 M ATP solutions respectively. Snapshots containing overlay of protein's conformations in absence of ATP (neat water) and in presence of ATP (0.5 M) are shown in figure G and H respectively. Protein is colored by secondary structure and ATP molecules in figure H are shown in line representation with an atom based coloring scheme (C: cyan, N: blue, O: red).

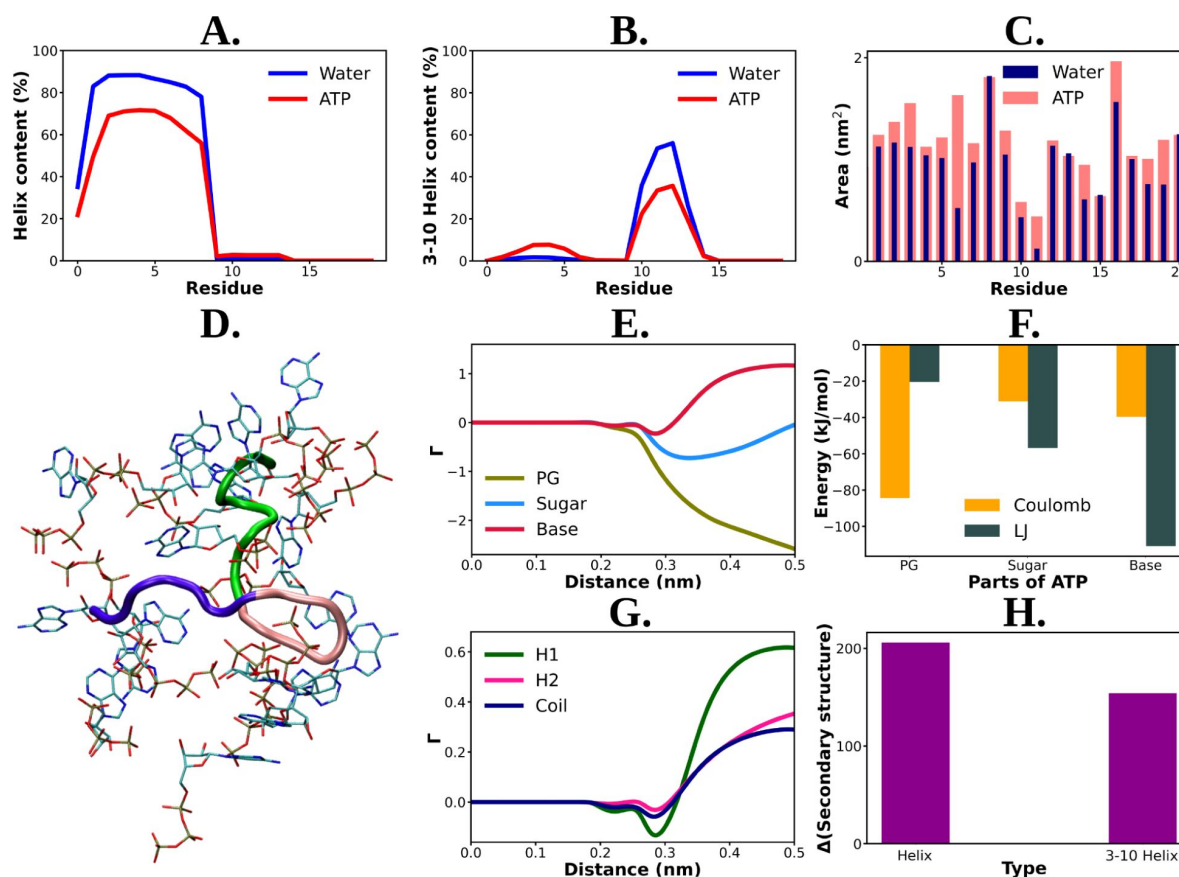


Figure 3

Residue wise total percentage of helix and 3-10 helix content of Trp-cage protein in absence and presence of ATP (0.5 M ATP) are shown in figure A and B respectively. Figure C. The solvent accessible surface area is calculated (with gromacs module of “gmx sasa”) for Trp-cage and represented for the aqueous medium without and with ATP corresponding to each of the protein residues in a bar plot representation. Figure D shows a representative snapshot of ATP’s (in licorice representation with atom based coloring scheme) interaction with Trp-cage (new cartoon representation. Green: H1 (1-9), pink: H2 (10-15), navy blue: coil (16-20)). E. Preferential interaction coefficient (r) of different parts of ATP: PG, sugar and base (with respect to solvent, water) with protein are being compared. F. Bar plot representation of coulombic and LJ interaction performed by all three different parts of ATP (PG, sugar and base) with Trp-cage. Figure G. represents the comparative plots of the preferential interaction coefficient (r) of ATP with the three structurally different parts (H1, H2 and coil) of Trp-cage. H. The change in the secondary structure content (helix and 3-10 helix) due to action of ATP are being represented. The difference in helix and 3-10 helix content in neat water from that of ATP solution are shown in bar plots.

base indicated that ATP's interaction with the protein is primarily driven by this moiety. This finding is supported by the hydrophobic nature of a significant fraction of Trp-cage residues (see **Figure 1** [↗](#) for a pie chart of residue) and the predominance of van der Waals interactions in the favorable base part of ATP-protein interaction (**figure 3 F** [↗](#)). The preferential interaction analysis also revealed that the base part of ATP interacts more strongly with the helix (H1) region of Trp-cage compared to the 3-10 helix (H2) and coil structures (see **Figure 3 G** [↗](#)). Consequently, the prominent interaction with the helical region results in a greater disruption of the helical structure (**Figure 3 H** [↗](#)) compared to others (3-10 helical or coil), leading to improved solubilization potential. These results provide valuable insights into the specific interactions between ATP and protein as the key for ATP's actions and also enhance our understanding of the interplay between ATP and protein structure.

ATP's impact on an Intrinsically Disordered Protein (IDP)

The observation of ATP's unfolding effect on a model globular protein across a range of concentrations encouraged us to explore how its impact would vary on an IDP Aβ40, which sits at the other end of the spectrum of protein family. Aβ40 has also remained a regular subject of pathological neurodegeneration due to its self-aggregation propensity. Accordingly, extensively long MD (30 μs) simulation trajectory of monomeric Aβ40 in 50 mM aqueous NaCl media, as obtained from D. E. Shaw research, was analyzed ¹⁶[↗](#). To realize the effect of ATP on the conformational ensemble of Aβ40, we simulated the conformational repertoire of the monomeric form of Aβ40 in 0.5 M aqueous ATP solution containing 50 mM NaCl salt. The former experiments investigating protein (unstructured) aggregation in presence of ATP, had been performed by maintaining ATP:protein stoichiometric ratio in the range of 0.1×10^3 to 1.6×10^3 , similarly we have also maintained ATP/protein stoichiometry 0.1×10^3 in our investigation ATP's effect on disordered protein Aβ40. The protein was modeled with CHARMM36m force field parameters and was solvated with TIP3P water molecules. To facilitate exhaustive sampling of Aβ40 in ATP medium, replica exchange MD (REMD) simulation was performed with a total 64 replicas in a temperature range of 290 to 460 K (see Method). A comparison of 2D free energy map (**Figure 4 A-B** [↗](#)) along R_g and the total number of inter-residue contact of Aβ40 in aqueous media (later referred as water) containing no ATP and that in presence of 0.5 M aqueous ATP (later referred as ATP) indicates a clear shift of relative population of Aβ40 conformational sub-ensemble towards a basin with higher R_g and lower number of contacts in presence of ATP, suggesting unfolding of the protein chain by ATP. To verify that the effect of ATP on conformational landscape is not an artifact of difference in sampling method (long conventional MD in absence of ATP versus REMD in presence of ATP), we repeated the conformational sampling in absence of ATP via employing REMD, augmented by adaptive sampling (figure S4). We find that the free energy map remains qualitatively similar (**figure 4A** [↗](#) and S4) irrespective the sampling technique. Comparison of 2D free energy map obtained from REMD simulation in absence of ATP (figure S4) with the one obtained in presence of ATP (**figure 4B** [↗](#)) also indicates ATP driven protein chain elongation. Representative snapshot of the conformation of Aβ40 in aqueous ATP media reveals significantly enhanced disorder in protein (**Figure 4 C** [↗](#)). Aβ40 is also very prone to form β-sheet in aqueous medium and thus gets associated in extensive protein aggregation. The central hydrophobic core (residue 17-21), (CHC) ¹⁷[↗](#) (shown in purple color in **Figure 1** [↗](#)) participates in the β-sheet formation in water and acts as the nucleating core during the pathogenesis relevant to Alzheimer's disease (AD). Interestingly, as evident from the snapshots and from the relative comparison of ensemble-averaged residue-wise β-sheet propensity (**Figure 4 D** [↗](#)), ATP reduces the content of β-sheet in CHC region and its partner β-fragment residue 30-35 (SHR, the secondary hydrophobic region). The decrease in the β-sheet signature in aqueous ATP solution is also apparent in the inter-residue contact map (**Figure 4 E-F** [↗](#)).

The presence of D23-K28 salt bridge ²[↗](#),¹⁸[↗](#),¹⁹[↗](#) has been previously reported in the Aβ40 monomer present within aqueous medium. This salt bridge interaction subsequently gives rise to a structural motif which is sufficiently potent for nucleation. D23-K28 salt bridge interaction in Aβ40 has remained crucial in the context of fibrillogenic activities conducted by the pathogenic

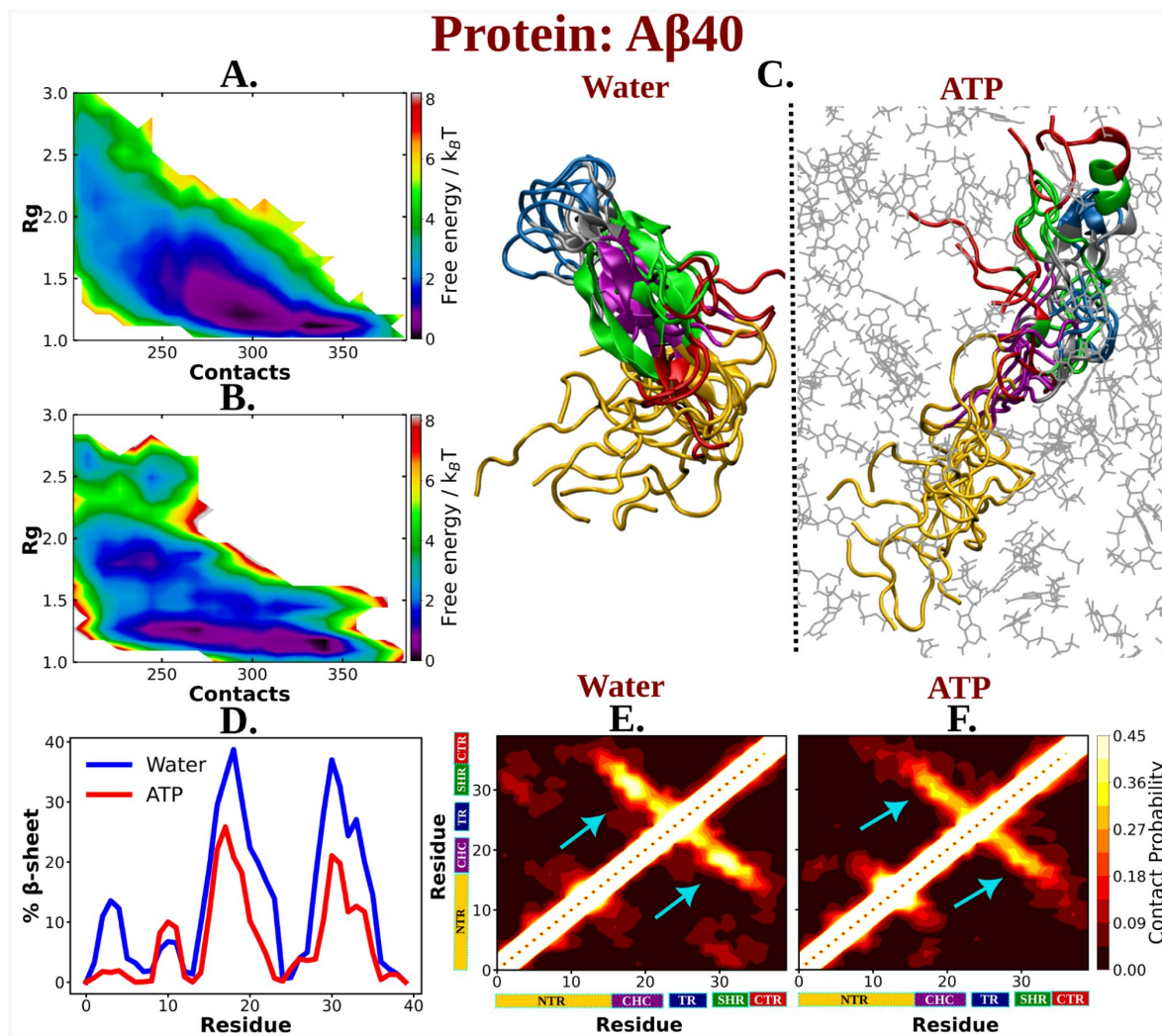


Figure 4

The 2D free energy profile of A β 40 monomer estimated with respect to R_g and total number of intra-chain contacts are shown in figure A and B for A β 40 in neat water and 0.5 M ATP respectively. Figure C. compares the simulation snapshots of A β 40 monomer in neat water and in presence of ATP. Multiple conformations are overlaid for each of the cases to represent the statistical significance. Protein is colored region wise as done in [Figure 1](#) and ATP molecules are shown by gray color line representation. Figure D. compares the β -sheet content of the A β 40 protein in water and in 0.5 M ATP solution. Figure E and F show the residue wise intra chain contact map of A β 40 in absence and in presence of ATP (0.5 M) respectively.

A β 40. The salt-bridge interaction of D23-K28 stabilizes the β -turn²⁰ in the region of V24-N27 which consequently favors the hydrophobic contacts between the central hydrophobic core (CHC) and the C-terminal part of A β 40. The structural bend in the zone of residue 23-28 through salt-bridge interaction helps the CHC (residue 17-21) and SHR fragments (residue 30-35) to adopt β -sheet formation which gets further stabilized with L17-I32 hydrophobic interaction^{2,18,19}. All these intramolecular interactions (salt-bridge interaction: D23-K28, β -turn: V24-N27, hydrophobic contact: L17-I32) within A β 40 protein in water, effectively result in the adoption of the β -structure which might be critically responsible for its higher propensity to form pathological amyloid fibrils^{2,18}.

The present simulation trajectory of monomeric A β 40 in 50 mM aqueous NaCl solution (water) traced all these aforementioned important fibrillogenic interactions. In particular in water the conformational ensemble of A β 40 adopted D23-K28 salt-bridge, V24-N27 β -turn and L17-I32 hydrophobic interaction (**Figure 5 A-F**), as evident from close pairwise distance of separation (see S5 A-C). These result in a constrained β -hairpin structure of A β 40 in water which is capable of inducing aggregation. In presence of ATP (0.5 M ATP in 50 mM NaCl solution), contacts present in these motifs get significantly disfavoured (**Figure 5 A-F** and S4 A-C), thereby substantially reducing the possibility of aggregation.

Interestingly, ATP's direct interaction (Figure S6) with the protein molecule allows the disruption of all these pathogenic molecular interactions. **Figure 5 G** represents the ATP's region specific (PG, sugar and base) interaction with the protein A β 40. The estimation of Coulombic and van der waal interaction energy indicates that unlike Trp-cage (**Figure 3 F**), Coulombic interaction of ATP with protein predominates in A β 40 (**Figure 5 H**), partly due to higher proportion of charge in this IDP (see the pie chart for A β 40 in **Figure 1**). This result signifies that ATP works in the protein specific manner.

An analysis of solvation free energy of the protein (see method) in absence and in presence of ATP predicted that the presence of ATP in aqueous solution significantly decreases the free energy required to solvate the IDP (**Figure 5 I**), hinting at the ATP's possible role in solubilizing the IDP. This was also evident in the ATP-induced increase in SASA of the protein (Figure S7).

Experimental Investigation of ATP's effect on aggregation of Nucleating core of A β 40

The aforementioned computer simulation predicts that ATP has the potential to decrease the beta-sheet content within the nucleating core of monomeric A β 40. This finding prompted us to conduct wet-lab experiments to investigate whether ATP plays a role in solubilizing the aggregation-prone A β content.

To explore experimental evidence of this influence on the dissolution of misfolded protein, we opted to focus on a shorter subset of the sequence rather than the entire sequence of the intrinsically disordered A β (1-40) amyloid. Consequently, we selected a short peptide stretch containing the important nucleating core of A β (1-40) from the 16th to the 22nd residue [Ac-KLVFFAE-NH₂, Ac-KE] involving the fibrillogenic CHC region (**Figure 6 A**)²¹, which had been suggested by aforementioned computer simulation to impart crucial contribution in formation of β -sheet conformation. This nucleating core is potentially known to act as the intermolecular glue during aggregation. Lysine at the N-terminal and glutamic acid at the C-terminal facilitated an antiparallel arrangement during assembly formation, contributing to colloidal stability²². To initiate the assembly of Ac-KE, the synthesized peptide was dissolved in a solution consisting of 40% acetonitrile-water containing 0.1% trifluoroacetic acid (TFA, pH 2). Following an incubation period of approximately 11-15 days, the assemblies exhibited a characteristic β -sheet structure, as revealed by circular dichroism (CD), resembling that of A β amyloid (Figure S8)²³.

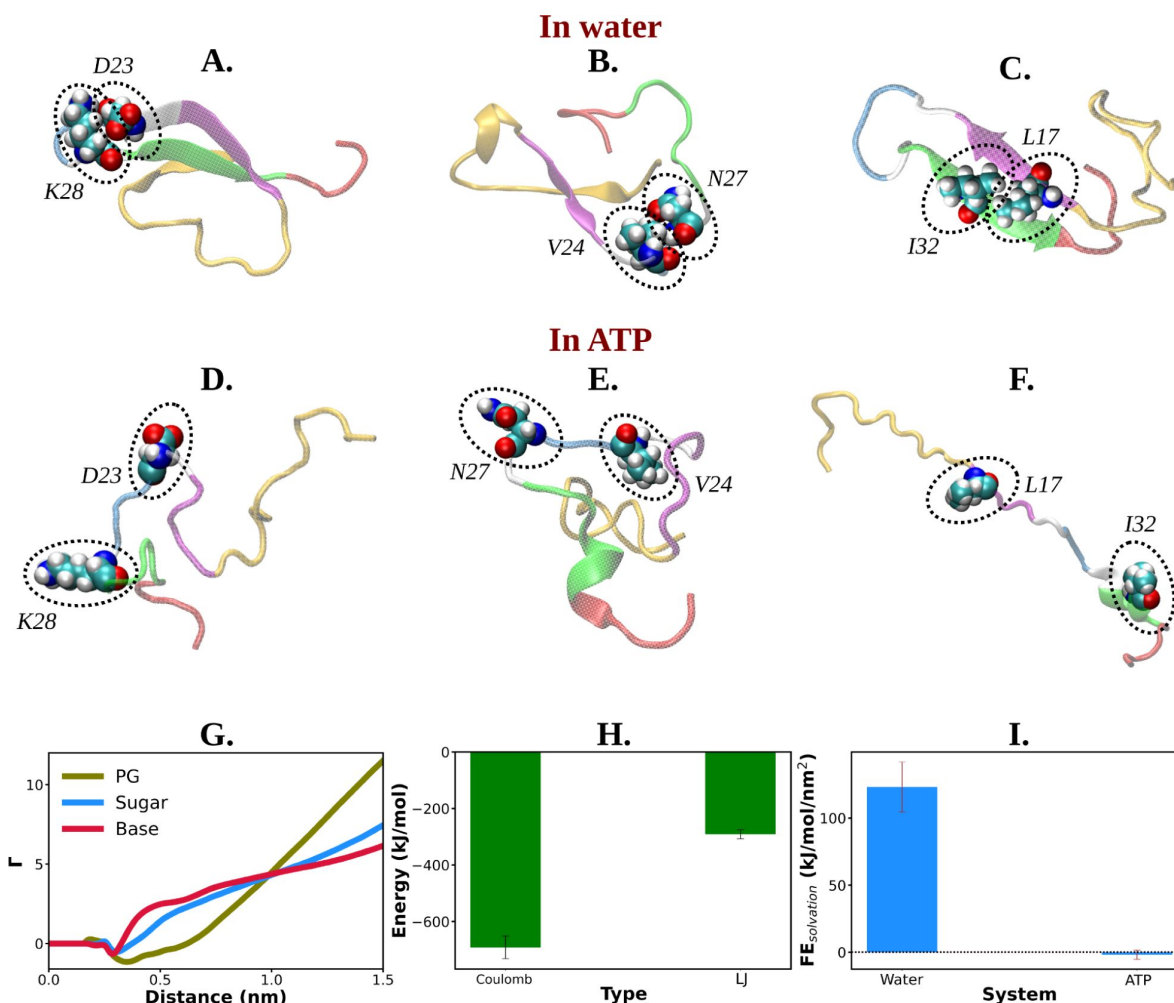


Figure 5

Figure A, B and C show the representative snapshots of different pairs of interacting residues namely, D23-K28, V24-N27 and L17-I32 respectively compared for salt water. The similar set of interactions are being represented in Figures D, E and F for ATP solution containing salt. G. Preferential interaction coefficient (Γ) of different parts of ATP (PG, sugar and base) with protein are being represented with respect to solvent water. H. The combined coulombic and LJ interaction energies imparted by all the three parts of ATP with A β 40 are shown. I. The free energy of solvation (calculated by the gromacs module of "gmX sasa") of A β 40 protein in absence and in presence of ATP are shown in a bar plot diagram. The vertical lines over the bars show the error bars.

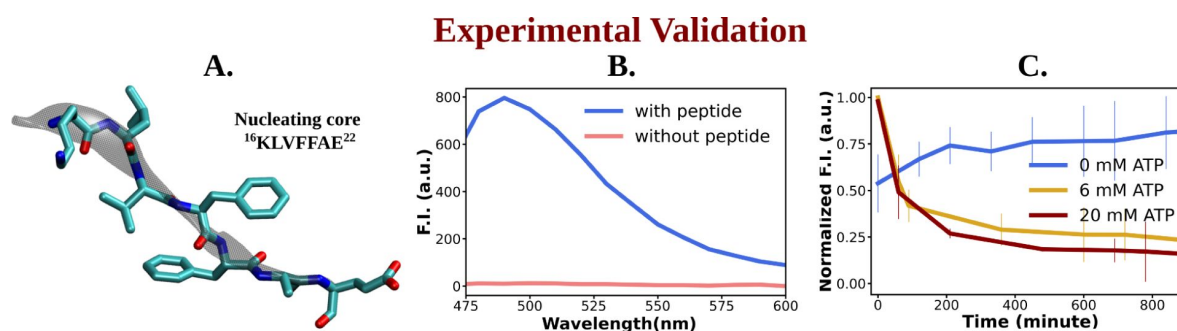


Figure 6

Figure A shows the representative snapshot of the peptide belonging to the nucleating core (16^{th} to 22^{nd} residue [Ac-KLVFFAE-NH₂, Ac-KE]) of the A β 40 protein, which is utilized for the experimental measurements. Figure B represents emission spectra of ThT in the presence (blue) and absence (pink) of peptide assembly in 10 mM HEPES buffer pH 7.2. Excitation wavelength (λ_{ex}) = 440 nm. (Final concentration [Ac-KE]=200 μM , [ThT]=30 μM). Figure C shows a comparative plot of ThT (30 μM) assay of AcKE (300 μM) assembly with time in 10 mM pH 7.2 HEPES buffer with 0 mM (blue curve), 6 mM (yellow curve) and 20 mM (dark red curve) of ATP. The vertical lines over the bars show the error bars.

The impact of ATP on amyloid fibrils was investigated using the Thioflavin T (ThT) assay, a well-established method for probing amyloid assembly (**Figure 6 B** [↗](#)). In presence of Ac-KE assembly, ThT demonstrated an intense emission at 480 nm which suggested the presence of preformed amyloid aggregation (**Figure 6 B** [↗](#))²⁴²⁵. Various AcKE:ATP ratios, ranging from 1:0 to 1:66.7, were tested in HEPES buffer (pH 7.2, 10 mM) at room temperature to assess the influence of ATP on preformed amyloid assemblies (Ac-KE). Interestingly, a progressive reduction in ThT intensity at 480 nm in the presence of ATP (**Figure 6C** [↗](#)) was observed over time, compared to the control system, which contained only the peptide assembly (Ac-KE) in a similar environment (**Figure 6C** [↗](#)). This decrease of ThT intensity in aqueous ATP solution reported the dissolution of the peptide assembly and disruption of the binding sites. Subsequently, morphological changes were examined using transmission electron microscopy (TEM) by casting the incubated samples on the TEM grid (see experimental measurement subsection in Method section). We expected that the investigation from electron microscopy would help in witnessing the visual transformation of fibrillar morphology in the presence of ATP. As a control experiment, the same concentration of Ac-KE assembly was also incubated without ATP in the similar environment for 18 h. Notably, micrographs recorded at different time frame supported the gradual dissolution of the peptide assembly when samples were incubated with ATP within 18 hours, while the control systems containing only Ac-KE did not demonstrate any noticeable alteration in their fibrillar morphologies (**Figure 7 A-C** [↗](#)), library of TEM micrographs: Figure S9-S11).

Molecular basis of ATP's solubilizing Role of Aβ40 aggregates

The experimental findings indicating ATP's potential role in solubilizing the fibrils of the Aβ40 nucleating core motivated us to explore the molecular basis through the early step of oligomerization. To investigate this, we conducted computational simulations of the dimerization process of Aβ40 in aqueous ATP (0.5 M) media containing 50 mM NaCl and compared it with the same aqueous condition without ATP. Initially, three configurations were considered by placing two copies of the protein at a distance (see methods), and unrestrained molecular dynamics (MD) simulations were performed under both conditions, with and without ATP.

The time profiles of the distance between inter-protein contact pairs (involving CHC-CHC, **Figure 8A** [↗](#), and involving CHC-SHR, **Figure 8B** [↗](#)) revealed that, within the simulation time frame, the pair of Aβ40 approached each other and formed a dimer. However, the propensity for Aβ40 dimerization was significantly diminished in aqueous ATP media. The residue-wise inter-protein contact map of Aβ40 in the absence and presence of ATP molecules (**Figure 8 C-D** [↗](#)) further illustrated the disappearance of multiple contact densities in the presence of ATP. Contacts such as CHC-CHC, CHC-SHR, and SHR-SHR²⁶ [↗](#), which were highly likely to form between protein pairs in aqueous saline medium, did not appear at all in the presence of ATP (**Figure 8 D** [↗](#)).

The nucleating core (involving the CHC region) of Aβ40, the same motif used in the previously described wet-lab experiment, played a crucial role as an intermolecular glue. Its active involvement in strong interactions with neighboring Aβ40 protein chains hindered the onset of protein aggregation via the first step of dimerization.

The direct interaction of ATP with Aβ40, playing a pivotal role in attenuating protein-protein interactions, is evident from the preferential interaction coefficient (Γ) of ATP (**Figure 8E** [↗](#)) with different parts of Aβ40 (NTR, CHC, TR, SHR, and CTR). Notably, ATP exhibits the strongest interactions with CHC and SHR (followed by NTR, TR, and CTR). These regions, as highlighted in the inter-residue contact map in the absence of ATP (**Figure 8C** [↗](#)), predominantly participate in inter-protein interactions during Aβ40 dimerization (refer to **Figure 8F** [↗](#) for a snapshot). A representative snapshot (**Figure 8G** [↗](#)) illustrates the effective crowding of ATP molecules around Aβ40, preventing protein copies from engaging in intermolecular interactions.

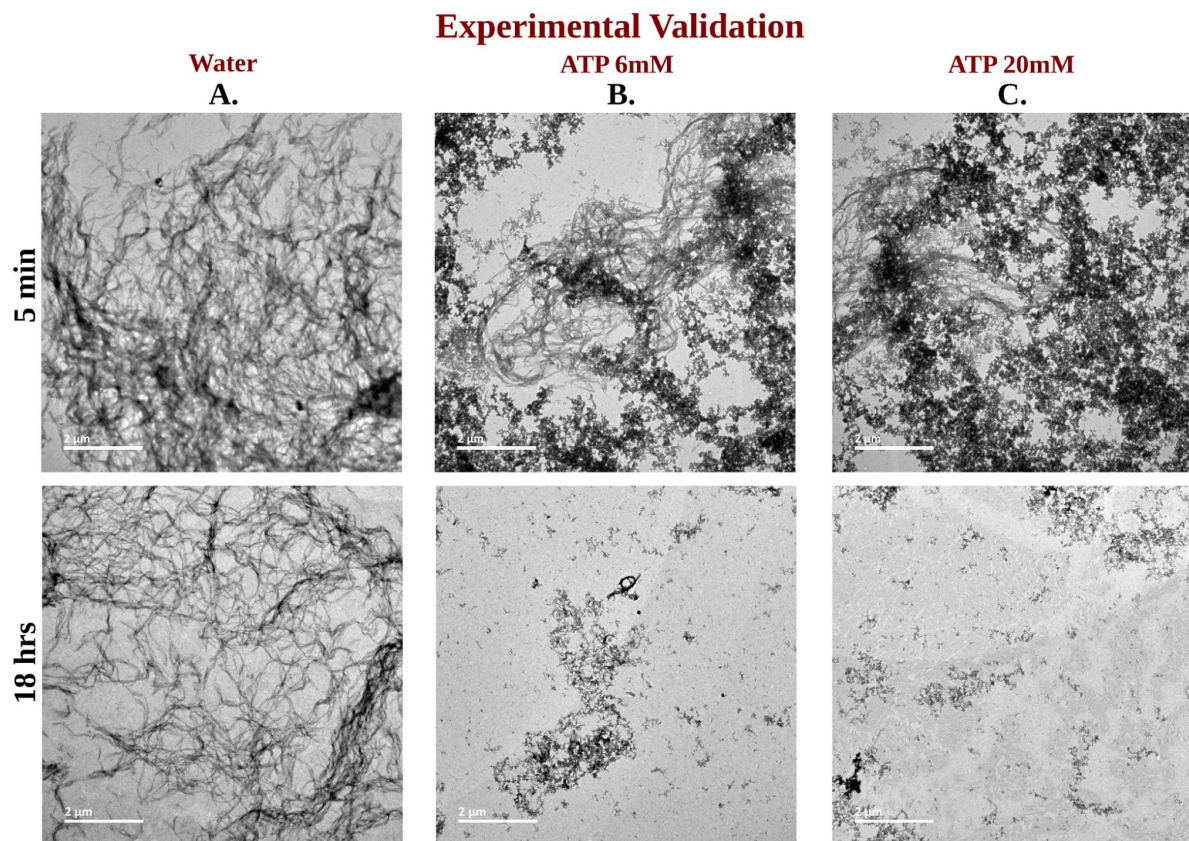


Figure 7

Library of TEM micrographs of Ac-KE (300 μ M) assemblies in 10 mM pH 7.2 HEPES buffer at 5 min (up) and after 18 h (down) of incubation, in presence of A. 0 mM ATP B. 6 mM ATP and C. 20 mM ATP are being represented.

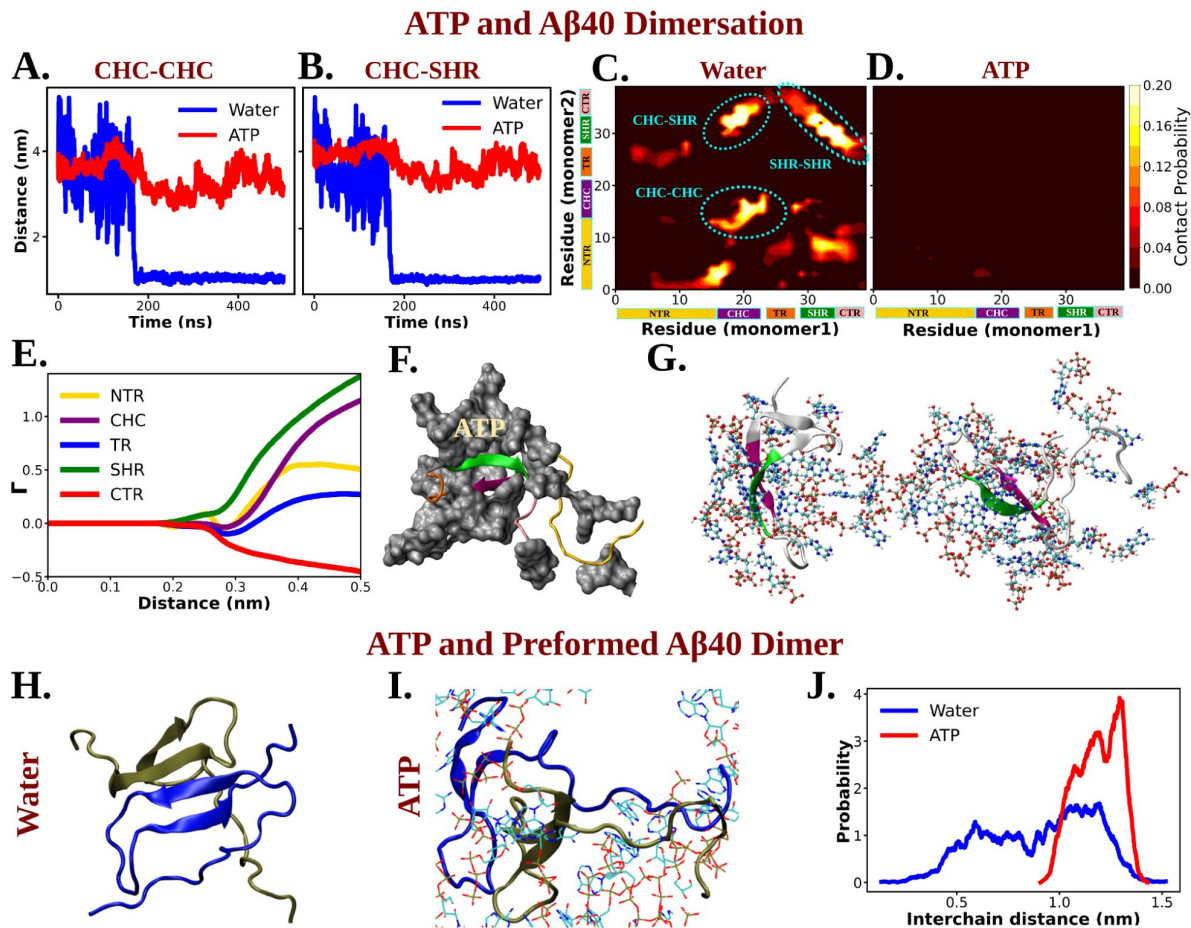


Figure 8

Figure A and B show the time profile of distance between the two actively interacting regions of two protein chains namely CHC-CHC and CHC-SHR respectively both in neat water and in presence of ATP co-solute (0.5 M ATP in 50 mM NaCl solution). Figure C and D represent residue-wise inter-protein contact map of A β 40 in water and in 0.5 M ATP solution respectively. The contacts (CHC-CHC, CHC-SHR, SHR-SHR) found in neat water are highlighted. Figure E. The preferential interaction coefficient (Γ) of ATP with each different part of A β 40 protein (NTR, CHC, TR, SHR and CTR) are being shown. F. Interaction of A β 40 protein chain with ATP cosolute. ATP molecules are being shown in vdw representation. G. The interacting ATP molecules crowd around the two A β 40 protein chains are being shown. Figure H and I show the consequence of A β 40 dimer in neat water and in presence of ATP respectively. The corresponding simulation snapshots are being shown for simulation starting with A β 40 dimer in water and in 0.5 M ATP in 50 mM NaCl solution. Figure J represents the probability distribution of distance between the two protein copies of the preformed A β 40 dimer in absence (50 mM NaCl solution) and presence of ATP (0.5 M ATP in 50 mM NaCl solution).

The preferential interaction of ATP can also help to lower the probability of intermolecular steric zipper type interaction (M35-M35) ²⁷, which plays a crucial role in aggregation. The inter-chain M35-M35 involving steric zipper interaction is important in forming amyloid fibrils by stabilizing sheet-to-sheet packing with the non-polar zipper. ATP can disrupt the steric-zipper interaction through its direct interaction (Figure S12 A) with M35 residue A β 40 as ATP makes it less available for intermolecular interaction through crowding (Figure S12 B).

ATP's solubilizing ability of preformed oligomers

ATP not only prevents protein aggregation but can also dissolve pre-existing protein droplets, effectively maintaining proteostasis within cells. To explore ATP's action on a preformed dimer, simulations were initiated with the already-formed protein dimer conformation and simulated its fate in a 50 mM NaCl solution, both with and without the presence of 0.5 M ATP in the same saline medium (Figure 8H-J). Interestingly, ATP was found to disrupt the dimer structure (Figure 8I), while the structure remained stable in the absence of ATP (Figure 8H). The probability distribution (Figure 8J) illustrates that, in the presence of ATP, the two protein chains, initially part of the dimer, become prone to be moved away from each other. This demonstrates that, in addition to inhibiting the formation of new protein aggregates, ATP is potent enough to disassemble existing protein droplets, maintaining proper cellular homeostasis. In summary, ATP has been observed to prevent protein condensation, dissolve previously formed condensates, and thereby enhance the solubility of biomolecules within aqueous cellular environments for proper cellular functions.

Is ATP special in its role as an aggregate solubilizer ?

A crucial question rises: Is ATP special in its role as an aggregate solubilizer? Towards this end, to investigate ATP's relative efficiency in inducing the solubility of hydrophobic entities (biological macromolecules) within cells, we compared it to a conventional chemical hydrotrope sodium xylene sulfonate (NaXS), routinely used in various industrial applications to solubilize sparingly soluble compounds in water. Simulations were conducted with two copies of A β 40 proteins in a 0.5 M NaXS solution, similar to those performed for 0.5 M ATP and 0 M ATP scenarios (discussed earlier; see methods for details).

Figure 9A illustrates the time profile of the distance between two protein monomers in 0.5 M NaXS solution compared with that in ATP solution (0.5 M) and neat water. Interestingly, ATP prevents the protein chains from coming closer to each other, while in NaXS solution, the proteins exhibit comparatively closer proximity. This trend is further emphasized by the probability distribution of the interprotein distance (Figure 9B), which shows a gradual decrease in the distance between protein chains from neat water to 0.5 M NaXS solution and finally to 0.5 M ATP. This suggests that, compared to NaXS, ATP is more efficient in enhancing solubility in aqueous medium by preventing the formation of aggregates.

For a quantitative assessment of ATP's efficiency over NaXS, we calculated the bound percentage of protein monomers in each of the three cases (Figure 9C). NaXS in water reduces the percentage of bound slightly, indicating a decrease in protein aggregation. However, ATP outperforms NaXS by significantly reducing the propensity of A β 40 dimerization.

The potency of ATP in inhibiting protein aggregation and maintaining solubility in an aqueous environment, compared to NaXS, is further evident from the estimation of the total number of interprotein contacts (Figure 9D). As we move from neat water to 0.5 M NaXS solution and finally to 0.5 M ATP solution, the number of intermolecular contacts between the two protein chains gradually decreases, highlighting ATP's efficiency over NaXS.

ATP vs chemical hydrotrope NaXS

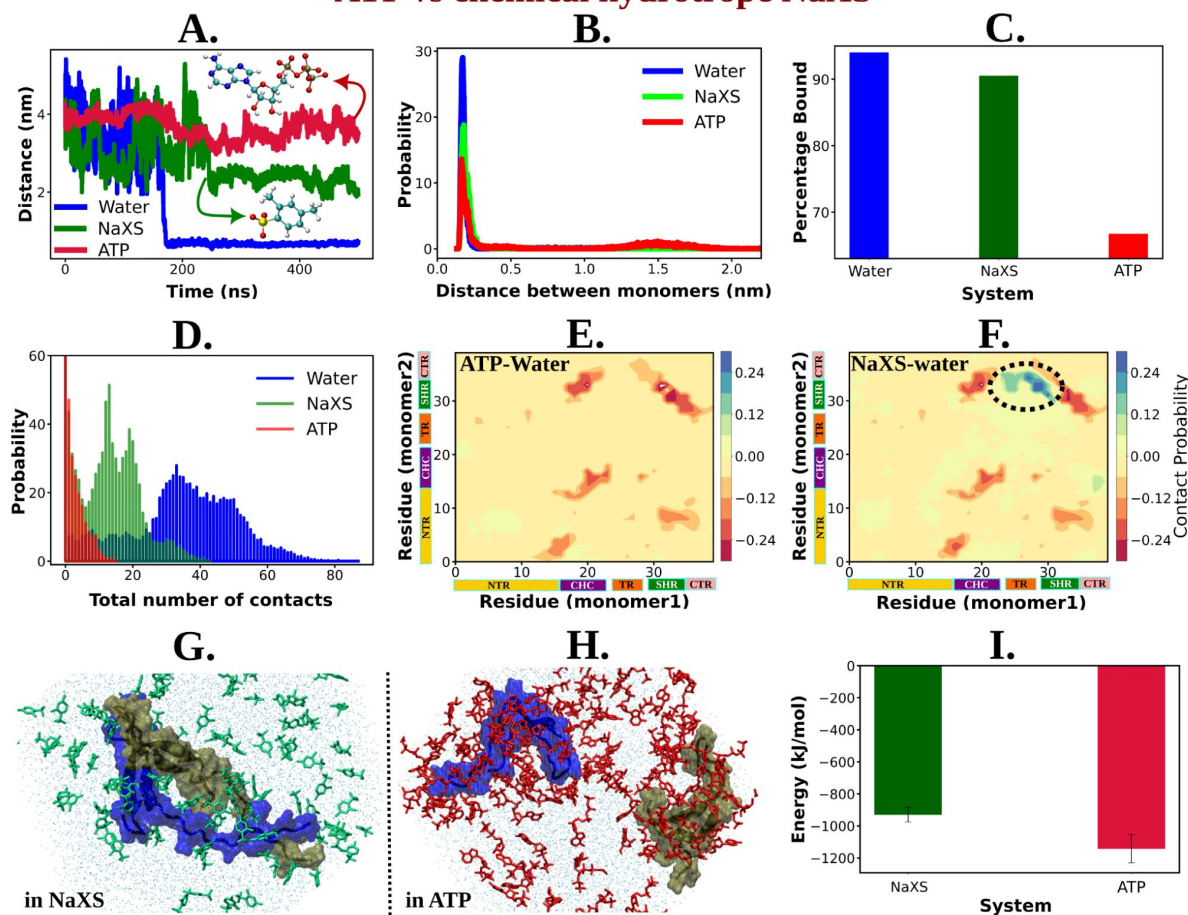


Figure 9

Figure A shows the time profile of distance between the two protein chains (CHC-CHC) in neat water (blue curve), in 0.5 M NaXS (green curve) and ATP (red curve) in 50 mM NaCl solution. Figure B represents the probability distribution of the distance between the protein chains in each of the three (above mentioned) cases. Figure C shows the percentage of bound of the proteins (for all the three systems) in a bar plot representation. Figure D depicts the total number of intermolecular contacts of the protein monomers in each of the three solutions. Figure E and F represent the difference of residue-wise inter-protein contact map of Aβ40 in 0.5 M ATP and 0.5 M NaXS solution respectively from that of the neat water system. Figure G and H show the representative snapshots captured during the Aβ40 dimerization simulation in 0.5 M NaXS and 0.5 M ATP solution respectively. Figure I represents the interaction energy (Coulombic interaction) between the NaXS (green bar) and ATP (red bar) molecules with the protein molecules in a bar plot representation. The vertical lines (black colored) show the error bars in the estimation.

The contact map (residue-wise inter protein contact map) difference (contact map of ATP/NaXS+water from that in neat water only) reveals that in the presence of ATP, there is a significant decrease in the probability of interprotein contacts (**Figure 9E**), a crucial factor in protein aggregation (**Figure 8C**). In contrast, in the presence of NaXS (**Figure 9F**), along with a decrease in some contact probabilities, there is an increase in interprotein contacts, especially involving the CHC and TR region of one chain with the SHR region of the other protein.

In nutshell, ATP acts more efficiently compared to NaXS by effectively inhibiting interprotein interactions, preventing aggregation, and maintaining protein solubility in an aqueous environment (**Figure 9G-H**). To elucidate the factors contributing to ATP's superiority over NaXS, we examined the interaction energy (Coulombic interaction) of both ATP and NaXS with the protein molecules (**Figure 9I**). The analysis revealed that, in comparison to NaXS, ATP exhibits a stronger interaction with the proteins, resulting in higher interaction energy. This heightened interaction energy plays a crucial role in preventing protein-protein interactions, ultimately leading to the effective inhibition of aggregation.

Comparing the effects of ATP with other nucleotides such as ADP and GTP, we emphasize that previous studies have demonstrated GTP can dissolve protein droplets (such as FUS) with efficiency comparable to ATP. However, in vivo, the concentration of GTP is significantly lower than that of ATP, resulting in negligible impact on the solubilization of liquid compartments. In contrast, ADP and AMP show much lower efficiency in dissolving protein condensates, indicating the critical role of the triphosphate moiety in protein condensate dissolution. Furthermore, only TP-Mg exhibited a negligible effect on protein droplet dissolution, suggesting that the charge density in the ionic ATP side chain alone is insufficient for this process. These findings underscore ATP's superior efficacy as a protein aggregate solubilizer, attributed to its specific chemical structure rather than merely its amphiphilicity.

Discussion and Conclusion

While previous efforts have explored ATP-driven protein disaggregation, its impact on protein conformational plasticity, crucial for self-assembly, is understudied. Our computational investigation prioritizes the examination of ATP's influence on protein conformational thermodynamics and correlates it with preventing protein aggregation. Regardless of biomolecular structure (globular or intrinsically disordered), ATP is found to induce protein chain extension, disrupting specific secondary structures and promoting flexibility for solvation in water. We demonstrate ATP's direct enhancement of protein aqueous solubility through calculations of solvation free energy and solvent-accessible surface area (SASA). The substantial increase in accessible surface area and more negative solvation free energy in aqueous ATP solution compared to ATP-free solution highlights ATP's pivotal role in preventing protein aggregation by increasing aqueous solubility through protein chain extension.

We followed up the simulation's prediction on ATP's role on protein conformation via a set of proof-of-concept experiments, in which we investigated ATP's impact on the fibrillogenic nucleating core of A β 40 (residues 16th to 22nd). ThT assays revealed a monotonically decreasing intensity over time with increasing ATP concentrations (0 mM to 20 mM), indicating the dissolution of A β 40 peptide assemblies. Transmission electron microscopy (TEM) confirmed the dissolution of peptide assemblies within 18 hours in ATP-treated samples, contrasting with control systems containing only Ac-KE, which showed no significant alteration in fibrillar morphologies. This experimental evidence, coupled with insights into ATP's role in enhancing aqueous solubility, necessitates an understanding of its molecular inhibitory mechanisms at the oligomerization level²⁸.

Computational studies focused on the primitive aggregation stage, specifically A β 40 dimerization, revealed that ATP disrupts dimer formation compared to the rapid dimerization observed in water. ATP's ability to guide conformational changes, particularly by disfavoring β -sheet adoption between the CHC and SHR fragments, efficiently inhibits A β 40 dimerization. Direct interactions between ATP molecules and the protein were identified as crucial, preventing pathological interactions (CHC-CHC, CHC-SHR, SHR-SHR) associated with the β -sheet motif. Additionally, ATP not only inhibits aggregation but also disintegrates previously formed dimers, highlighting its capability to dissolve existing protein aggregates. Overall, ATP's multifaceted action, from inhibiting dimerization to disrupting existing dimers, underscores its potential in preventing pathological protein aggregation.

In conclusion, beyond its role in various energetic modulations, ATP contributes significantly and independently of energy expenditure to the proper functioning of proteins in crowded cellular environments with high salt concentrations, mitigating biomolecular instabilities linked to diseases involving pathological protein aggregation. Our study demonstrates that ATP's micromanagement starts at the protein monomeric level, orchestrating conformational modifications to ensure adequate aqueous solubility. By perturbing intramolecular contacts, ATP induces structural flexibility, facilitating effective water solubilization of protein monomers. Simultaneously, ATP discourages the adoption of fibrillogenic protein conformations prone to aggregation. Recently described as hydrotropic activity, our findings provide a detailed understanding of the biological rationale for the exceptionally high concentration of ATP in cells compared to other nucleotides, as reported by Patel et al.¹ While previous studies highlighted ATP's antiaggregation property, our investigation elucidates its mechanism: ATP's remarkable influence on protein conformational modification helps hydrophobic protein molecules remain favorably soluble in the cellular aqueous medium, thereby reducing their propensity for self-aggregation. Overall, ATP's regulatory role in conformational plasticity emerges as a key factor behind its hydrotropic function in biological systems.

The mechanistic details of ATP's interaction with proteins have been subjected to various interpretations. Few studies proposed a nonspecific ATP-protein interaction^{3,29}, contrasting with the some reports explaining ATP's preferential binding to conserved residues (Arg and Lys or Tyr and Ser)^{4,6,30}. Some studies highlighted ATP's role as a solvation mediator with the capabilities of ATP in hydrophobic, π - π , π -cation, and electrostatic interactions with proteins^{2,9,10,31}. In our investigation, we found that ATP interacts directly with Trp-cage and A β 40 proteins in a protein-specific manner, utilizing its chemically distinct parts—negatively charged PG group, hydrophilic sugar moiety, and hydrophobic aromatic base—to engage in electrostatic, H-bond-like, and hydrophobic interactions with protein residues. The nature of ATP's interactions varies significantly based on the amino-acid composition of the protein. For the hydrophobic Trp-cage, ATP favors van der Waals' interactions over electrostatic ones, while for the charged A β 40, Coulombic interactions dominate. This protein-dependent specificity enhances ATP's efficiency in cellular processes, aligning with recent proteome-wide² studies showing diverse effects of ATP on protein thermal stability and solubility. Notably, intrinsically disordered proteins experience enhanced solubility with ATP, while some proteins exhibit decreased solubility.

In our literature survey of ATP's concentration-dependent actions, as detailed in the Introduction section, we observed a dual role where ATP induces protein liquid-liquid phase separation at lower concentrations and promotes protein disaggregation at higher concentrations^{6,32,33}. These versatile functions emphasize ATP's pivotal role in maintaining a delicate balance between protein stability (at low ATP concentrations) and solubility (at high ATP concentrations) for effective proteostasis within cells. Notably, ATP-mediated stabilization primarily targets soluble proteins, particularly those with ATP-binding motifs, while ATP-driven biomolecular solubilization is observed for insoluble proteins, typically lacking ATP-binding motifs. The question arises: how does ATP selectively stabilize or destabilize proteins? Recent proteome-based² investigations

align with previous study³⁴ indicating that ATP predominantly stabilizes soluble bio-molecules, especially those featuring the P-loop motif (GK[X]nS/T or G[X]nK[X]nK). Our Sequence-based analysis of reported proteins, including ubiquitin, malate dehydrogenase, and TDP-43 RRM domain, reveals conservation of the P-loop motif in their respective ATP-recognition site (see SI). Conversely, proteins like Trp-cage and A β 40, undergoing ATP-driven solubilization at the expense of conformational stability, lack the P-loop motif (see SI). This suggests that ATP deciphers information from the primary structure (protein sequence) to govern secondary and tertiary structures, selectively stabilizing ATP-binding proteins and inducing solubilization in the absence of ATP-binding motifs during protein unfolding.

In summary, while previous reports emphasize ATP's role in inhibiting protein aggregation, our work connects these findings by highlighting ATP's influence starting at the monomeric level, thereby preventing proteins from becoming aggregation-prone. The distinctive protein-dependent and region-specific interactions between ATP and protein molecules play a pivotal role in regulating protein structure. This interaction mechanism leads to an exceptionally efficient inhibition of protein aggregation compared to conventional chemical hydrotropes. ATP orchestrates a two-stage hydrotropic action, from monomer destabilization to early-stage aggregation prevention. The necessity for higher cellular concentrations of ATP underscores its significance, potentially explaining the frequent onset of protein aggregation-related diseases with aging, attributed to ATP deficiency. The collaborative efforts of simulation and experimentation in this study suggest potential implications and therapeutic interventions using ATP for future treatments of various neurodegenerative diseases.

Method and Materials

A. Simulation model and methods

In this work, we have studied the effect of ATP on the conformational plasticity of two different types of proteins belonging from the contrasting protein spectrum: 1. folded globular protein, Trp-cage which stands as one of the very suitable prototypical computational mini-protein models with less charge content and 2. the intrinsically disordered protein, A β 40 containing higher proportion charged residues (in line with the typical nature of IDP), which is popularly known for its characteristic high aggregation propensity (**Figure 1**). Here we have individually investigated the conformational dynamics of both the proteins in absence and presence of ATP-Mg²⁺. The folded protein Trp-cage, PDB: 1L2Y, (both the N and C terminal of the protein was capped with acetyl group and methyl amide respectively) was studied in neat water and in 0.1 M and 0.5 M aqueous ATP solution (protein/ATP stoichiometry of 0.02*10³). Further equivalent number of Mg²⁺ ions were incorporated into the simulation box. The system was charge neutralized with an equivalent number of chloride ions. The protein was modeled with a99SB-*disp* forcefield parameters and solvated with TIP4P-*disp* water molecules¹⁶. The ion parameters were taken from a99SB-*disp* forcefield. During simulation with ATP-Mg²⁺ (0.1 M and 0.5 M), ATP molecules were modeled with Amber force field parameters. For Trp-cage simulations in neat water and 0.5 M ATP-Mg²⁺ aqueous solution the box volume was 4.4*4.4*3.1 nm³ and for 0.1 M ATP-Mg²⁺ simulation with Trp-cage the box dimension was kept fixed as 8.2*8.2*5.7 nm³.

First each system was energy-minimized followed by two consecutive steps of equilibration: 1. NVT equilibration for 1 ns at an equilibrium temperature of 300 K utilizing the Nosé–Hoover thermostat³⁵³⁶ (1 ps time constant) and then 2. equilibration in NPT ensemble for 2 ns at 300 K temperature and 1 bar pressure maintained using the Nosé–Hoover thermostat (time constant of 1 ps) and Berendsen barostat³⁷ (time constant of 1.0 ps) respectively. Further the system was again equilibrated in the NPT ensemble for 10 ns at an equilibrium temperature of 300 K and an equilibrium pressure of 1 bar, maintained by employing the Nosé–Hoover thermostat (time constant of 1 ps) and the Parrinello–Rahman barostat³⁸ (time constant of 1.0 ps) respectively.

The particle-mesh Ewald (PME)^{38,39} method with a grid spacing of 0.12 nm was applied for managing long-range electrostatics. For constraining the bonds associated with hydrogen atoms and the bonds and angle of water molecules, the LINCS method⁴⁰ and SETTLE algorithm^{40,41} respectively were used. To perform all the molecular dynamics (MD) simulations GROMACS⁴² software of version 2018.6 software was utilized.

To ensure exhaustive exploration of protein conformational landscape conditions, each condition (Trp-cage in neat water and 0.1 M and 0.5 M ATP-Mg²⁺ aqueous solution of Trp-cage) was simulated via Replica exchange molecular dynamics (REMD) simulation⁴³. For performing REMD simulation the former equilibrated systems were employed. REMD simulation was done in the temperature range of 280–540 K with a total of 54 replicas (for 0.1 M ATP-Mg²⁺ solution the temperature range was 290–460 K with 64 replicas). At first each of the replicas was well equilibrated for 5 ns in the NVT ensemble at the respective replica temperature employing the Nosé–Hoover thermostat (time constant 1 ps). Eventually the production simulations were performed for 400 ns (250 ns for 0.1 M ATP-Mg²⁺ solution of Trp-cage) at each replica with a replica exchange interval of 10 ps. Finally the trajectory corresponding to the replica temperature of 303 K was considered for subsequent analysis. Further to test the robustness of our estimation across the choice of force field, the similar set of simulations for the Trp-cage protein in neat water and in 0.5 M ATP are performed with Charmm 36 force field parameters for protein⁴⁴ and ATP⁴⁵ and using Charmm TIP3P water model^{10,46}. For these simulations in the Charmm36 force field the similar simulation protocol has been utilized.

Apart from folded globular protein, for studying ATP's effect on the conformation plasticity of an intrinsically disordered protein we have chosen Aβ40 which is routinely investigated in the context of protein aggregation related pathogenic conditions. Accordingly, the 30 us long MD simulation trajectory of monomeric Aβ40 in 50 mM aqueous NaCl media, from D. E. Shaw research was utilized¹⁶. To realize the impact of ATP on the conformational dynamics of Aβ40, we simulated the conformational repotiere of monomeric form of Aβ40 (initial structure same as D. E. Shaw research group) in 0.5 M (ATP/protein stoichiometry 0.1*10³) aqueous ATP solution containing 50 mM NaCl salt. At first the protein was incorporated in the simulation box of dimension 8.2*8.2*5.7 nm³ followed by addition of ATP molecules to maintain ATP concentration of 0.5 M. Equivalent numbers of Mg²⁺ ions were added. Finally the system was solvated with water molecules sufficient to fill up the box. The protein was modeled with charmm36m force field parameters¹⁶ and for water molecules, Charmm TIP3P water model was employed^{10,46}. The ion parameters are obtained from the Charmm 36m forcefield. ATP molecule is modeled with Charmm36 force field parameters⁴⁵. For exhaustive sampling of the protein in ATP medium, REMD simulation was performed with a total 64 replicas in a temperature range of 290 to 460 K. Each of the replicas were simulated for 400 ns at the replica exchange interval of 10 ps, leading to a cumulative sampling aggregate equivalent to around 26 microseconds. The REMD conformations corresponding to 303 K were further clustered into 213 clusters via the R_g and total number of inter-residue contacts of the protein chain based on regular space clustering algorithm. Finally, 213 independent MD simulations were performed for 100 ns (each) with the different initial configurations (Aβ monomer dissolved in 0.5 M ATP in 50 mM aqueous NaCl solution) chosen randomly from individual clusters. The concatenated short trajectories were employed for generating 2D energy profiles and for all other calculation 303 K REMD simulation trajectory was employed. The 213 short MD simulation trajectories are used separately for building a Markov state model (MSM)⁴⁷ in order to statistically map the complete process of protein conformational change using PyEMMA software^{47,48}. From MSM, the stationary populations of the discrete microstates were calculated and eventually utilized for reweighing the free energy surfaces obtained from these short trajectories. To test the robustness we have also estimated the 2D free energy profile of Aβ40 in absence of ATP by performing similar REMD simulation followed by adaptive sampling simulation following the similar protocol described above.

Further to test the correlation of ATP's effect on protein monomeric level with its potency to inhibit aggregation, we have carried out equilibrium dimer simulations with the aggregation prone amyloidogenic protein $\alpha\beta 40$. We have started our simulation from three different conformations involving the protein chains at three different distances 1 nm, 2 nm and 4 nm. Two replica simulations are performed with each of the configurations for 500 ns following the similar simulation protocol as mentioned above. The similar set of dimer simulations were performed for the two copies of the $\alpha\beta 40$ proteins in the 50 mM aqueous NaCl solution and also 0.5 M aqueous ATP solution containing 50 mM NaCl salt. The same box size was maintained for each of the dimer simulations as $8.2 \times 8.2 \times 5.7 \text{ nm}^3$ (same as the monomeric $\alpha\beta 40$ simulation with ATP-Mg^{2+}). Later we have repeated the similar dimer simulations for 0.5 M NaXS in the 50 mM aqueous NaCl solution, following the similar simulation protocol.

To assess the impact of ATP on the pre-existing protein droplets, we have tested ATP's effect on the preformed dimer. We have started our simulation with preformed $\alpha\beta 40$ dimer (three dimer conformations were obtained from the previously described $\alpha\beta 40$ dimerization simulation in 50 mM NaCl salt solution and simulations were carried out corresponding to each of the dimer conformation) dissolved in 0.5 M ATP-Mg^{2+} in 50 mM aqueous NaCl solution. Simulation was performed in the same box size of $8.2 \times 8.2 \times 5.7 \text{ nm}^3$ following the similar simulation protocol. Simulation was continued up to 1 μs .

GROMACS software analysis tools were utilized for computing the radius of gyration (R_g), number of hydrogen bonds of the proteins. The fraction of native contacts (for Trp-cage) was estimated using PLUMED software⁴⁹ with a cutoff of 0.7 nm. For calculating the total number of contacts and residue-wise contact map MDAAnalysis⁵⁰ tool was employed along with python scripting. The secondary structure content of each of the proteins was estimated using the STRIDE program of VMD. The calculation of the solvent accessible surface area was performed with the help of the GROMACS analysis tool (gmx sasa). The 2D free energy profiles were computed for each of the systems using the PyEMMA tool. The hydrophobicity index of each of the proteins was obtained from the peptide 2.0 web server "https://www.peptide2.com/N_peptide_hydrophobicity_hydrophilicity.php". For quantitative estimation of ATP's interaction with the proteins, the Wyman–Tanford preferential interaction coefficient^{51,52} (Γ_s) was calculated^{53–55} with respect to water.

$$\Gamma_s = \left\langle n_s - \frac{N_s^{\text{tot}} - n_s}{N_w^{\text{tot}} - n_w} \cdot n_w \right\rangle$$

where n_s is the number of cosolute bound with the protein molecule and N^{tot} is the total number of the species present within the system. n_w represents the number of water molecules bound to the surface of the protein and N^{tot} is the total number of water of the system.

B. Experimental Measurements: Materials

All protected amino acids, activator N,N'-Diisopropylcarbodiimide (DIC), N,N-diisopropylethylamine (DIPEA), Trifluoroacetic acid (TFA), piperidine, Uranyl acetate, Thioflavin T and HEPES were purchased from Sigma Aldrich. Oxyma was purchased from Nova Biochem. All solvents and Fmoc-Rink amide MBHA Resin were purchased from Merck. Milli-Q water was used throughout the experiments.

Peptide Synthesis and Characterization

Ac-KLVFFAE-NH₂ (Ac-KE) peptide was synthesized by solid phase peptide synthesizer (CEM Liberty Blue). Fmoc-Rink Amide MBHA resin (loading 0.52 mmol/g) was swollen using dimethylformamide (DMF) for 15 min, followed by Fmoc deprotection with 20% piperidine in DMF. Each Fmoc-amino acid coupling step was performed using DIC and oxyma pure in DMF. Subsequently, acetylation of the N-terminus lysine was done using acetic anhydride in DMF. The resin was washed with dichloromethane (DCM) after completion of the final coupling and allowed to dry in open air.

Peptide was cleaved from the resin using TFA/triethyl silane (5:0.1 v/v) solution for 2 h, followed by precipitation in cold diethyl ether after removing the TFA. The product was centrifuged at 5000 rpm for 15 min at 4 °C in Eppendorf centrifuge 5804 R and further, the pellet was washed 3 times with cold diethyl ether. Molecular mass was confirmed by Waters Xevo G2-XS QTof.

Ac-KLVFFAE-NH₂ (Ac-KE) (C₄₅H₆₇N₉O₁₀) (m/z) calculated for [M+H⁺]: 894.50; found: 894.52

Peptide assembly

The dried powder of the peptide (Ac-KLVFFAE-NH₂) was treated with HFIP to eliminate preformed assembly during precipitation in ether. After that, HFIP was removed through N₂ blowing and the peptide film was dissolved in 40 % acetonitrile-water containing 0.1 % Trifluoroacetic acid through vortexing and sonication. The homogeneous solution of peptide was kept for 11-15 days at ambient temperature (~2-8 °C) to form assembly formation.

Circular Dichroism

A JASCO J-810 circular dichroism spectrometer fitted with a Peltier temperature controller to maintain the temperature at 25 °C was used to record the CD spectra. 200 μM of Ac-KE (stock 2.5 mM) aged assemblies was taken in Mili-Q water and the spectra were recorded in a quartz cuvette with a 1 mm path length. Spectrum was recorded throughout the wavelength range from 300 nm to 180 nm with a scan rate of 100 nm/min and two accumulations.

Thioflavin T assay

The 11-15 days matured assembly Ac-KE peptide (300 μM) was mixed with different concentrations of ATP (6 and 20 mM) in 10 mM of HEPES buffer (pH 7.2) at room temperature. 30 μM of ThT dye was added to the mixture and started the experiment with excitation wavelength (λ_{ex}) at 440 nm and emission (λ_{em}) at 480 nm. Kinetics was recorded for 18 h with 30 min intervals, and 30 sec constant shaking was set before taking the data. The gain was fixed to 50 in the microplate reader (BioTek, SYNERGY H1). To check the control, only Ac-KE (300 μM) was taken in a similar environment and data were recorded.

To check ThT as a reporter for amyloid assembly fluorescence spectra in microplate reader was checked for 200 μM of Ac-KE assembly in presence of 30 μM ThT. The excitation wavelength and gain were set at 440 nm and 50 respectively.

References

- (1) Patel A., Malinowska L., Saha S., Wang J., Alberti S., Krishnan Y., Hyman A. A. (2017) **ATP as a Biological Hydrotrope** *Science* **356**:753–756
- (2) Sridharan S., Kurzawa N., Werner T., Günthner I., Helm D., Huber W., Bantscheff M., Savitski M. (2019) **Proteome-Wide Solubility and Thermal Stability Profiling Reveals Distinct Regulatory Roles for ATP** *Nat. Commun* **10**
- (3) Nishizawa M., Walinda E., Morimoto D., Kohn B., Scheler U., Shirakawa M., Sugase K. (2021) **Effects of Weak Nonspecific Interactions with ATP on Proteins** *J. Am. Chem. Soc* **143**:11982–11993
- (4) Kim T. H., Payliss B. J., Nosella M. L., Lee I. T. W., Toyama Y., Forman-Kay J. D., Kay L. E. (2021) **Interaction Hot Spots for Phase Separation Revealed by NMR Studies of a CAPRIN1 Condensed Phase** *Proc. Natl. Acad. Sci. U. S. A* **118** <https://doi.org/10.1073/pnas.2104897118>
- (5) Ou X., Lao Y., Xu J., Wutthinitikornkit Y., Shi R., Chen X., Li J. (2021) **ATP Can Efficiently Stabilize Protein through a Unique Mechanism** *JACS Au* **1**:1766–1777
- (6) Song J. (2021) **Adenosine Triphosphate Energy-Independently Controls Protein Homeostasis with Unique Structure and Diverse Mechanisms** *Protein Sci* **30**:1277–1293
- (7) He Y., Kang J., Song J. (2020) **ATP Antagonizes the Crowding-Induced Destabilization of the Human Eye-Lens Protein γ S-Crystallin** *Biochem. Biophys. Res. Commun* **526**:1112–1117
- (8) Aida H., Shigeta Y., Harada R. (2022) **The Role of ATP in Solubilizing RNA-Binding Protein Fused in Sarcoma** *Proteins* **90**:1606–1612
- (9) Pal S., Paul S. (2020) **ATP Controls the Aggregation of A β Peptides** *J. Phys. Chem. B* **124**:210–223
- (10) Sarkar S., Mondal J. (2021) **Mechanistic Insights on ATP's Role as a Hydrotrope** *J. Phys. Chem. B* **125**:7717–7731
- (11) Hayes M. H., Peuchen E. H., Dovichi N. J., Weeks D. L. (2018) **Dual Roles for ATP in the Regulation of Phase Separated Protein Aggregates in Oocyte Nucleoli** *eLife* **7** <https://doi.org/10.7554/eLife.35224>
- (12) Greiner J. V., Glonek T. (2021) **Intracellular ATP Concentration and Implication for Cellular Evolution** *Biology* **10** <https://doi.org/10.3390/biology10111166>
- (13) Sarkar S., Narayanan T. N., Mondal J. (2023) **A Synergistic View on Osmolyte's Role against Salt and Cold Stress in Biointerfaces** *Langmuir* **39**:17581–17592
- (14) Ahalawat N., Mondal J. (2018) **Assessment and Optimization of Collective Variables for Protein Conformational Landscape: GB1 -Hairpin as a Case Study** *J. Chem. Phys* **149**

- (15) Menon S., Adhikari S., Mondal J. (2024) **An Integrated Machine Learning Approach Delineates Entropy-Mediated Conformational Modulation of α -Synuclein by Small Molecule** *eLife* **13** <https://doi.org/10.7554/elife.97709.1>
- (16) Robustelli P., Piana S., Shaw D. E. (2018) **Developing a Molecular Dynamics Force Field for Both Folded and Disordered Protein States** *Proc. Natl. Acad. Sci. U. S. A* **115**:E4758–E4766
- (17) Jana A. K., Batkulwar K. B., Kulkarni M. J., Sengupta N. (2016) **Glycation Induces Conformational Changes in the Amyloid- β Peptide and Enhances Its Aggregation Propensity: Molecular Insights** *Phys. Chem. Chem. Phys* **18**:31446–31458
- (18) Tarus B., Straub J. E., Thirumalai D. (2006) **Dynamics of Asp23-Lys28 Salt-Bridge Formation in Abeta10-35 Monomers** *J. Am. Chem. Soc* **128**:16159–16168
- (19) Sgourakis N. G., Yan Y., McCallum S. A., Wang C., Garcia A. E. (2007) **The Alzheimer's Peptides Abeta40 and 42 Adopt Distinct Conformations in Water: A Combined MD / NMR Study** *J. Mol. Biol* **368**:1448–1457
- (20) Larini L., Shea J.-E. (2012) **Role of β -Hairpin Formation in Aggregation: The Self-Assembly of the Amyloid- β (25-35) Peptide** *Biophys. J* **103**:576–586
- (21) Mehta A. K., Lu K., Childers W. S., Liang Y., Dublin S. N., Dong J., Snyder J. P., Pingali S. V., Thiyagarajan P., Lynn D. G. (2008) **Facial Symmetry in Protein Self-Assembly** *J. Am. Chem. Soc* **130**:9829–9835
- (22) Hsieh M.-C., Lynn D. G., Grover M. A. (2017) **Kinetic Model for Two-Step Nucleation of Peptide Assembly** *J. Phys. Chem. B* **121**:7401–7411
- (23) Harada T., Kuroda R. (2011) **CD Measurements of β -Amyloid (1-40) and (1-42) in the Condensed Phase** *Biopolymers* **95**:127–134
- (24) Sulatskaya A. I., Kuznetsova I. M., Turoverov K. K. (2011) **Interaction of Thioflavin T with Amyloid Fibrils: Stoichiometry and Affinity of Dye Binding, Absorption Spectra of Bound Dye** *J. Phys. Chem. B* **115**:11519–11524
- (25) Biancalana M., Makabe K., Koide A., Koide S. (2009) **Molecular Mechanism of Thioflavin-T Binding to the Surface of Beta-Rich Peptide Self-Assemblies** *J. Mol. Biol* **385**:1052–1063
- (26) Fatafta H., Khaled M., Owen M. C., Sayyed-Ahmad A., Strodel B. (2021) **Amyloid- β Peptide Dimers Undergo a Random Coil to β -Sheet Transition in the Aqueous Phase but Not at the Neuronal Membrane** *Proc. Natl. Acad. Sci. U. S. A* **118** <https://doi.org/10.1073/pnas.2106210118>
- (27) Zheng J., Jang H., Ma B., Tsai C.-J., Nussinov R. (2007) **Modeling the Alzheimer Abeta17-42 Fibril Architecture: Tight Intermolecular Sheet-Sheet Association and Intramolecular Hydrated Cavities** *Biophys. J* **93**:3046–3057
- (28) Kurisaki I., Tanaka S. (2019) **ATP Converts A β Oligomer into Off-Pathway Species by Making Contact with Its Backbone Atoms Using Hydrophobic Adenosine** *J. Phys. Chem. B* **123**:9922–9933
- (29) Zalar M., Bye J., Curtis R. (2023) **Nonspecific Binding of Adenosine Triphosphate and Triphosphate Modulates the Phase Behavior of Lysozyme** *J. Am. Chem. Soc* **145**:929–943

- (30) Coskuner O., Murray I. V. J. (2014) **Adenosine Triphosphate (ATP) Reduces Amyloid- β Protein Misfolding in Vitro** *J. Alzheimers. Dis* **41**:561–574
- (31) Dec R., Jaworek M. W., Dzwolak W., Winter R. (2023) **Liquid-Droplet-Mediated ATP-Triggered Amyloidogenic Pathway of Insulin-Derived Chimeric Peptides: Unraveling the Microscopic and Molecular Processes** *J. Am. Chem. Soc* <https://doi.org/10.1021/jacs.2c12611>
- (32) Ren C.-L., Shan Y., Zhang P., Ding H.-M., Ma Y.-Q. (2022) **Uncovering the Molecular Mechanism for Dual Effect of ATP on Phase Separation in FUS Solution** *Sci Adv* **8**
- (33) Liu F., Wang J. (2023) **ATP Acts as a Hydrotrope to Regulate the Phase Separation of NBDY Clusters** *JACS Au* **3**:2578–2585
- (34) Saraste M., Sibbald P. R., Wittinghofer A. (1990) **The P-Loop--a Common Motif in ATP- and GTP-Binding Proteins** *Trends Biochem. Sci* **15**:430–434
- (35) Nosé S. (1984) **A Molecular Dynamics Method for Simulations in the Canonical Ensemble** *Mol. Phys* **52**:255–268
- (36) Hoover W. G. (1985) **Canonical Dynamics: Equilibrium Phase-Space Distributions** *Phys. Rev. A Gen. Phys* **31**:1695–1697
- (37) Berendsen H. J. C., Grigera J. R., Straatsma T. P. (1987) **The Missing Term in Effective Pair Potentials** *J. Phys. Chem* **91**:6269–6271
- (38) Parrinello M., Rahman A. (1981) **Polymorphic Transitions in Single Crystals: A New Molecular Dynamics Method** *J. Appl. Phys* **52**:7182–7190
- (39) Darden T., York D., Pedersen L. (1993) **Particle Mesh Ewald: An N·log(N) Method for Ewald Sums in Large Systems** *J. Chem. Phys* **98**:10089–10092
- (40) Hess B. (2008) **P-LINCS: A Parallel Linear Constraint Solver for Molecular Simulation** *J. Chem. Theory Comput* **4**:116–122
- (41) Miyamoto S., Kollman P. A. (1992) **Settle: An Analytical Version of the SHAKE and RATTLE Algorithm for Rigid Water Models** *J. Comput. Chem* **13**:952–962
- (42) Abraham M. J., Murtola T., Schulz R., Páll S., Smith J. C., Hess B., Lindahl E. (2015) **GROMACS: High Performance Molecular Simulations through Multi-Level Parallelism from Laptops to Supercomputers** *SoftwareX* :19–25
- (43) Sugita Y., Okamoto Y. (1999) **Replica-Exchange Molecular Dynamics Method for Protein Folding** *Chem. Phys. Lett* **314**:141–151
- (44) Best R. B., Zhu X., Shim J., Lopes P. E. M., Mittal J., Feig M., Mackerell A. D. (2012) **Optimization of the Additive CHARMM All-Atom Protein Force Field Targeting Improved Sampling of the Backbone ϕ , ψ and Side-Chain $\chi(1)$ and $\chi(2)$ Dihedral Angles** *J. Chem. Theory Comput* **8**:3257–3273
- (45) Hart K., Foloppe N., Baker C. M., Denning E. J., Nilsson L., Mackerell A. D. (2012) **Optimization of the CHARMM Additive Force Field for DNA: Improved Treatment of the BI/BII Conformational Equilibrium** *J. Chem. Theory Comput* **8**:348–362

- (46) MacKerell A. D. *et al.* (1998) **All-Atom Empirical Potential for Molecular Modeling and Dynamics Studies of Proteins** *J. Phys. Chem. B* **102**:3586–3616
- (47) Husic B. E., Pande V. S. (2018) **Markov State Models: From an Art to a Science** *J. Am. Chem. Soc* **140**:2386–2396
- (48) Scherer M. K., Trendelkamp-Schroer B., Paul F., Pérez-Hernández G., Hoffmann M., Plattner N., Wehmeyer C., Prinz J.-H., Noé F. (2015) **PyEMMA 2: A Software Package for Estimation, Validation, and Analysis of Markov Models** *J. Chem. Theory Comput* **11**:5525–5542
- (49) Tribello G. A., Bonomi M., Branduardi D., Camilloni C., Bussi G. (2014) **PLUMED 2: New Feathers for an Old Bird** *Comput. Phys. Commun* **185**:604–613
- (50) Gowers R. *et al.* (2016) **MAnalysis: A Python Package for the Rapid Analysis of Molecular Dynamics Simulations** *In Proceedings of the 15th Python in Science Conference; SciPy* <https://doi.org/10.25080/majora-629e541a-00e>
- (51) Wyman J. (1964) **LINKED FUNCTIONS AND RECIPROCAL EFFECTS IN HEMOGLOBIN: A SECOND LOOK** *Adv. Protein Chem* **19**:223–286
- (52) Tanford C. (1969) **Extension of the Theory of Linked Functions to Incorporate the Effects of Protein Hydration** *J. Mol. Biol* **39**:539–544
- (53) Sarkar S., Guha A., Narayanan T. N., Mondal J. (2022) **Zwitterionic Osmolytes Revive Surface Charges under Salt Stress via Dual Mechanisms** *J. Phys. Chem. Lett* **13**:5660–5668
- (54) Sarkar S., Guha A., Sadhukhan R., Narayanan T. N., Mondal J. (2023) **Osmolytes as Cryoprotectants under Salt Stress** *ACS Biomater Sci Eng* **9**:5639–5652
- (55) Mondal J., Halverson D., Li I. T. S., Stirnemann G., Walker G. C., Berne B. J. (2015) **How Osmolytes Influence Hydrophobic Polymer Conformations: A Unified View from Experiment and Theory** *Proc. Natl. Acad. Sci. U. S. A* **112**:9270–9275

Editors

Reviewing Editor

Qiang Cui

Boston University, Boston, United States of America

Senior Editor

Qiang Cui

Boston University, Boston, United States of America

Reviewer #1 (Public review):

Summary:

This work combines molecular dynamics (MD) simulations along with experimental elucidation of the efficacy of ATP as biological hydrotrope. While ATP is broadly known as the energy currency, it has also been suggested to modulate the stability of biomolecules and their aggregation propensity. In the computational part of the work, the authors demonstrate that ATP increases the population of the more expanded conformations (higher radius of

gyration) in both a soluble folded mini-protein Trp-cage and an intrinsically disordered protein (IDP) A β 40. Furthermore, ATP is shown to destabilise the pre-formed fibrillar structures using both simulation and experimental data (ThT assay and TEM images). They have also suggested that the biological hydrotrope ATP has significantly higher efficacy as compared to the commonly used chemical hydrotrope sodium xylene sulfonate (NaXS).

Strengths:

This work presents a comprehensive and compelling investigation of the effect of ATP on the conformational population of two types of proteins: globular/folded and IDP. The role of ATP as an "aggregate solubilizer" of pre-formed fibrils has been demonstrated using both simulation and experiments. They also elucidate the mechanism of action of ATP as a multi-purpose solubilizer in a protein-specific manner. Depending on the protein, it can interact through electrostatic interactions (for predominantly charged IDPs like A β 40), or primarily van der Waals' interactions through (for Trp-Cage).

Weaknesses:

The weaknesses and suggestions mentioned in my first review have been adequately addressed by the authors in the revised version of the manuscript.

<https://doi.org/10.7554/eLife.99150.2.sa2>

Reviewer #3 (Public review):

Since its first experimental report in 2017 (Patel et al. Science 2017), there have been several studies on the phenomenon in which ATP functions as a biological hydrotrope of protein aggregates. In this manuscript, by conducting molecular dynamics simulations of three different proteins, Trp-cage, Abeta40 monomer, and Abeta40 dimer at concentrations of ATP (0.1, 0.5 M), which are higher than those at cellular condition (a few mM), Sarkar et al. find that the amphiphilic nature of ATP, arising from its molecular structure consisting of phosphate group (PG), sugar ring, and aromatic base, enables it to interact with proteins in a protein-specific manner and prevents their aggregation and solubilize if they aggregate. The authors also point out that in comparison with NaXS, which is the traditional chemical hydrotrope, ATP is more efficient in solubilizing protein aggregates because of its amphiphilic nature.

Trp-cage, featured with hydrophobic core in its native state, is denatured at high ATP concentration. The authors show that the aromatic base group (purine group) of ATP is responsible for inducing the denaturation of helical motif in the native state.

For Abeta40, which can be classified as an IDP with charged residues, it is shown that ATP disrupts the salt bridge (D23-K28) required for the stability of beta-turn formation.

By showing that ATP can disassemble preformed protein oligomers (Abeta40 dimer), the authors suggest that ATP is "potent enough to disassemble existing protein droplets, maintaining proper cellular homeostasis," and enhancing solubility.

Overall, the message of the paper is clear and straightforward to follow. In addition to the previous studies in the literature on this subject. (J. Am. Chem. Soc. 2021, 143, 31, 11982-11993; J. Phys. Chem. B 2022, 126, 42, 8486-8494; J. Phys. Chem. B 2021, 125, 28, 7717-7731; J. Phys. Chem. B 2020, 124, 1, 210-223), the study, which tested using MD simulations whether ATP is a solubilizer of protein aggregates, deserves some attention from the community and is worth publishing.

Weakness

My only major concern is that the simulations were performed at unusually high ATP concentrations (100 and 500 mM of ATP), whereas the real cellular concentration of ATP is 1-5 mM.

I was wondering if there is any report on a titration curve of protein aggregates against ATP, and what is the transition mid-point of ATP-induced solubility of protein aggregates. For instance, urea or GdmCl have long been known as the non-specific denaturants of proteins, and it has been well experimented that their transition mid-points of protein unfolding are in the range of $\sim(1 - 6)$ M depending on the proteins.

The authors responded to my comment on ATP concentration that because of the computational issue in all-atom simulations, they had no option but to employ mM-protein concentrations instead of micromolar concentrations, thus requiring 1000-folds higher ATP concentration, which is at least in accordance with the protein/ATP stoichiometry. However, I believe this is an issue common to all the researchers conducting MD simulations. Even if the system is in the same stoichiometric ratio, it is never clear to me (is it still dilute enough?) whether the mechanism of solubilization of aggregate at 1000 fold higher concentration of ATP remains identical to the actual process.

<https://doi.org/10.7554/eLife.99150.2.sa1>

Author response:

The following is the authors' response to the current reviews.

Reviewer #1 (Public review):

Summary:

This work combines molecular dynamics (MD) simulations along with experimental elucidation of the efficacy of ATP as biological hydrotrope. While ATP is broadly known as the energy currency, it has also been suggested to modulate the stability of biomolecules and their aggregation propensity. In the computational part of the work, the authors demonstrate that ATP increases the population of the more expanded conformations (higher radius of gyration) in both a soluble folded mini-protein Trp-cage and an intrinsically disordered protein (IDP) A β 40. Furthermore, ATP is shown to destabilise the pre-formed fibrillar structures using both simulation and experimental data (ThT assay and TEM images). They have also suggested that the biological hydrotrope ATP has significantly higher efficacy as compared to the commonly used chemical hydrotrope sodium xylene sulfonate (NaXS).

Strengths:

This work presents a comprehensive and compelling investigation of the effect of ATP on the conformational population of two types of proteins: globular/folded and IDP. The role of ATP as an "aggregate solubilizer" of pre-formed fibrils has been demonstrated using both simulation and experiments. They also elucidate the mechanism of action of ATP as a multi-purpose solubilizer in a protein-specific manner. Depending on the protein, it can interact through electrostatic interactions (for predominantly charged IDPs like A β 40), or primarily van der Waals' interactions through (for Trp-Cage).

Weaknesses:

The weaknesses and suggestions mentioned in my first review have been adequately addressed by the authors in the revised version of the manuscript.

Thank you very much for your positive feedback and for taking the time to thoroughly review our manuscript. Your thoughtful comments and suggestions have significantly contributed to enhancing the quality of our work.

We sincerely appreciate your time and efforts in helping us refine our research.

Reviewer #3 (Public review):

Since its first experimental report in 2017 (Patel et al. Science 2017), there have been several studies on the phenomenon in which ATP functions as a biological hydrotrope of protein aggregates. In this manuscript, by conducting molecular dynamics simulations of three different proteins, Trp-cage, Abeta40 monomer, and Abeta40 dimer at concentrations of ATP (0.1, 0.5 M), which are higher than those at cellular condition (a few mM), Sarkar et al. find that the amphiphilic nature of ATP, arising from its molecular structure consisting of phosphate group (PG), sugar ring, and aromatic base, enables it to interact with proteins in a protein-specific manner and prevents their aggregation and solubilize if they aggregate. The authors also point out that in comparison with NaXS, which is the traditional chemical hydrotrope, ATP is more efficient in solubilizing protein aggregates because of its amphiphilic nature.

Trp-cage, featured with hydrophobic core in its native state, is denatured at high ATP concentration. The authors show that the aromatic base group (purine group) of ATP is responsible for inducing the denaturation of helical motif in the native state.

For Abeta40, which can be classified as an IDP with charged residues, it is shown that ATP disrupts the salt bridge (D23-K28) required for the stability of beta-turn formation.

By showing that ATP can disassemble preformed protein oligomers (Abeta40 dimer), the authors suggest that ATP is "potent enough to disassemble existing protein droplets, maintaining proper cellular homeostasis," and enhancing solubility.

Overall, the message of the paper is clear and straightforward to follow. In addition to the previous studies in the literature on this subject. (J. Am. Chem. Soc. 2021, 143, 31, 11982-11993; J. Phys. Chem. B 2022, 126, 42, 8486-8494; J. Phys. Chem. B 2021, 125, 28, 7717-7731; J. Phys. Chem. B 2020, 124, 1, 210-223), the study, which tested using MD simulations whether ATP is a solubilizer of protein aggregates, deserves some attention from the community and is worth publishing.

Weakness

My only major concern is that the simulations were performed at unusually high ATP concentrations (100 and 500 mM of ATP), whereas the real cellular concentration of ATP is 1-5 mM.

I was wondering if there is any report on a titration curve of protein aggregates against ATP, and what is the transition mid-point of ATP-induced solubility of protein aggregates. For instance, urea or GdmCl have long been known as the non-specific denaturants of proteins, and it has been well experimented that their transition mid-points of protein unfolding are in the range of $\sim(1 - 6)$ M depending on the proteins.

The authors responded to my comment on ATP concentration that because of the computational issue in all-atom simulations, they had no option but to employ mM-protein concentrations instead of micromolar concentrations, thus requiring 1000-folds higher ATP concentration, which is at least in accordance with the protein/ATP stoichiometry. However, I believe this is an issue common to all the researchers conducting MD simulations. Even if the system is in the same stoichiometric ratio, it is

never clear to me (is it still dilute enough?) whether the mechanism of solubilization of aggregate at 1000 fold higher concentration of ATP remains identical to the actual process.

Thank you for your thoughtful feedback and for recognizing the value of our study. We appreciate your detailed review and the constructive comments you have provided.

We appreciate your understanding of the inherent limitations in MD simulations. The use of higher ATP concentrations in our simulations stems from the computational challenges of all-atom MD simulations. Due to the practical constraints of simulating micromolar protein concentrations in atomistic detail, we employed millimolar protein concentrations, which necessitated the use of ATP concentrations that are proportionally higher to maintain appropriate stoichiometry between ATP and proteins.

We fully agree with your point that this is a common issue faced by researchers in the MD simulation community. While it is challenging to directly replicate physiological ATP concentrations in atomistic simulations, we believe that our approach still captures the fundamental interactions between ATP and proteins. In particular, our focus was on the relative behaviors and mechanistic insights, rather than absolute concentration effects. We based our choice of ATP concentration on maintaining stoichiometric ratios with the protein concentration to ensure that the molecular mechanisms observed remain relevant. We hope our clarification addresses your concerns.

We would like to share that in an ongoing study focused on the role of ATP in influencing the liquid-liquid phase separation behavior of several intrinsically disordered proteins, we are employing a coarse-grained model. This approach allows us to maintain ATP concentrations within physiologically relevant ranges, as simulating micromolar protein concentrations becomes computationally feasible with this method. We believe that this complementary work will provide additional insights into the behavior of ATP at concentrations more reflective of cellular conditions and further validate the findings from our current study.

We would also like to emphasize that the complementary experiments presented in this study were conducted at physiologically relevant concentrations for both protein and ATP. The experimental results are in strong agreement with our computational findings, supporting the hypothesis that the mechanisms observed in the simulations closely reflect the actual biological process.

The following is the authors' response to the original reviews.

Reviewer #1 (Public Review):

Summary:

This work combines molecular dynamics (MD) simulations along with experimental elucidation of the efficacy of ATP as a biological hydrotrope. While ATP is broadly known as the energy currency, it has also been suggested to modulate the stability of biomolecules and their aggregation propensity. In the computational part of the work, the authors demonstrate that ATP increases the population of the more expanded conformations (higher radius of gyration) in both a soluble folded mini-protein Trp-cage and an intrinsically disordered protein (IDP) Aβ40. Furthermore, ATP is shown to destabilise the pre-formed fibrillar structures using both simulation and experimental data (ThT assay and TEM images). They have also suggested that the biological hydrotrope ATP has significantly higher efficacy as compared to the commonly used chemical hydrotrope sodium xylene sulfonate (NaXS).

Strengths:

This work presents a comprehensive and compelling investigation of the effect of ATP on the conformational population of two types of proteins: globular/folded and IDP. The role of ATP as an "aggregate solubilizer" of pre-formed fibrils has been demonstrated using both simulation and experiments. They also elucidate the mechanism of action of ATP as a multi-purpose solubilizer in a protein-specific manner. Depending on the protein, it can interact through electrostatic interactions (for predominantly charged IDPs like A β 40), or primarily van der Waals' interactions through (for Trp-Cage).

Weaknesses:

The data presented by the authors are sound and adequately support the conclusions drawn by the authors. However, there are a few points that could be discussed or elucidated further to broaden the scope of the conclusions drawn in this work as discussed below:

(i) The concentration of ATP used in the simulations is significantly higher (500 mM) as compared to those used in the experiments (6-20 mM) or cellular cytoplasm (~5 mM as mentioned by the authors). Since the authors mention already known concentration dependence of the effect of ATP, it is worth clarifying the possible limitations and implications of the high ATP concentrations in the simulations.

We thank the reviewer for their concern regarding the ATP concentration used in our simulation. The reviewer correctly noted our statement about cellular ATP concentrations being in the range of a few millimolar. We would like to highlight that, in a cellular environment, millimolar ATP concentrations coexist with micromolar protein concentrations in the aqueous phase [1].

In our study, we focused on the impact of ATP on protein conformational dynamics, primarily simulating a protein monomer within the simulation box. If one was required to maintain a micromolar protein concentration (e.g., 20 μ M [1]) for a monomeric protein, a MD simulation box of significant dimensions (~44x44x44 nm³) would be required, which is computationally challenging to simulate at an atomistic resolution due to the excessive computational cost and time. We had observed a severe reduction of performance of simulation (with Gromacs software of version 2018.6) of more than 150 times for the 20 μ M A β 40 protein in 20 mM ATP solution containing 50 mM NaCl salt which is comprised in the simulation box of ~ 44x44x44 nm³ in comparison to the current simulation set up we have employed in our study).

To ensure computational efficiency, we employed a simulation protocol that would maintain the cellular protein/ATP stoichiometry. Similar to the stoichiometry in the cellular environment (i.e., micromolar protein : millimolar ATP ~ 103), our simulations maintained a consistent ratio (i.e., millimolar protein : molar ATP ~ 103). This approach allowed us to use a smaller simulation box while preserving the relevant stoichiometry, enabling us to leverage data within a realistic timeframe.

Based on the reviewer comment we have included the explanation in the revised manuscript as "In this study, we opted to maintain the ATP stoichiometry consistent with biological conditions and previous in vitro experiments. Instead of keeping the protein concentration within the micromolar range and ATP concentration at the millimolar level, we chose this approach to avoid the need for an extremely large simulation box, which would greatly reduce computational efficiency by more than 150-fold." (page 4).

However, during our experimental measurements we have maintained micromolar concentration of protein and ATP concentration in the millimolar range, which lies consistent with the former in vitro experimental studies [1].

It seems ATP can stabilise the proteins at low concentrations, but the current work does not address this possible effect. It would be interesting to see whether the effect of ATP on globular proteins and IDPs remains similar even at lower ATP concentrations.

We thank the reviewer for raising this point. We would like to refer you to the Discussion and Conclusion sections of our manuscript (on page 18), where we have noted ATP's concentration-dependent actions on protein homeostasis, incorporating insights from previous literature as well: "In our literature survey of ATP's concentration-dependent actions, as detailed in the Introduction section, we observed a dual role where ATP induces protein liquid-liquid phase separation at lower concentrations and promotes protein disaggregation at higher concentrations [2–4]. These versatile functions emphasize ATP's pivotal role in maintaining a delicate balance between protein stability (at low ATP concentrations) and solubility (at high ATP concentrations) for effective proteostasis within cells. Notably, ATP-mediated stabilization primarily targets soluble proteins, particularly those with ATP-binding motifs, while ATP-driven biomolecular solubilization is observed for insoluble proteins, typically lacking ATP-binding motifs." We explain that ATP stabilizes proteins at lower concentrations, primarily targeting those with ATP-binding motifs, as illustrated by a sequence-dependent analysis. Since the proteins we studied (Trp-cage and A β 40) do not contain any ATP-binding motifs, ATP-guided protein stabilization is not expected for these proteins. Additionally, we presented a set of simulations for Trp-cage with a comparatively lower concentration of ATP (see Figure 2), which also suggests

ATP-driven protein chain elongation. Thus, we believe that ATP's effect on globular proteins and intrinsically disordered proteins (IDPs) lacking ATP-binding motifs would remain similar at lower ATP concentrations."

(ii) The authors make a somewhat ambitious statement that the role of ATP as a solubilizer of pre-formed fibrils could be used as a therapeutic strategy in protein aggregation-related diseases. However, it is not clear how it would be so since ATP is a promiscuous substrate in several biochemical processes and any additional administration of ATP beyond normal cellular concentration (~5 mM) could be detrimental.

The authors thank the reviewer for this comment. In conjunction with earlier studies on the non-energetic effects of ATP, our study underscores ATP's anti-aggregation properties and its ability to dissolve preformed aggregates, thereby maintaining regular protein homeostasis within cells and inhibiting protein aggregation-related diseases. Consequently, ATP has been proposed as a probable therapeutic agent in multiple previous reports [5–8]. Patel et al. also noted that as ATP levels decrease with age, this can lead to increased protein aggregation and neurodegenerative decline [1]. Therefore, the problem of excessive protein aggregation in cells may be linked to the reduction of ATP levels with aging [1,8–12]. In such circumstances, authors hypothesize introducing ATP as part of a therapeutic treatment might address the issue of excessive protein aggregation and neurodegenerative diseases.

(iii) A natural question arises about what is so special about ATP as a solubilizer. The authors have also asked this question but in a limited scope of comparing to a commonly used chemical hydrotrope NaXS. However, a bigger question would be what kind of chemical/physical features make ATP special? For example, (i) if the amphiphilic property is important, what about some standard surfactants? (ii) how would ATP compare to other nucleotides like ADP or GTP? It might be useful to explore such questions in the future to further establish the special role of ATP in this regard.

We thank the reviewer for recognizing the significance and value of our exploration into the unique properties of ATP as a solubilizer. In response to the reviewer's comment regarding the specific features that make ATP special, we would like to emphasize our analysis of ATP's region-specific interactions with biomolecules. ATP's unique structure, comprising three distinct moieties- a larger hydrophobic aromatic base, a hydrophilic sugar moiety, and a highly negatively charged phosphate group, enables it to perform multiple modes of interactions, including hydrophobic, hydrogen bonding, and electrostatic interactions with proteins. This combination of interactions leads to its pronounced effect in a protein-specific manner. We believe that, together with its amphiphilic property, the specific chemical structure of ATP makes it an efficient solubilizer. A previous study by Patel et al. demonstrated the efficiency of ATP as a biological hydrotrope compared to other classical chemical hydrotropes (NaXS and NaTO). Our current study further rationalizes ATP's efficiency through its effective interactions with biomolecules, driven by the chemically distinct parts of the ATP molecule.

Regarding the reviewer's point about comparing ATP as a hydrotrope with standard surfactants, we would like to add that typically, hydrotropes are amphiphilic molecules that differ from classical surfactants due to their low cooperativity of aggregation and their effectiveness at molar concentrations. Hydrotropes tend to preferentially accumulate non stoichiometrically around the solute, and their aggregation depends on the presence of solute molecules. Unlike surfactants, hydrotropes do not form any well-defined superstructure on their own.

In response to the reviewer's comment on comparing ATP's effect with other nucleotides like ADP and GTP, we would like to highlight that previous studies have shown GTP to dissolve protein droplets (FUS) with similar efficiency to ATP. However, in cells, the concentration of GTP is much lower than that of ATP, resulting in negligible effects on the solubilization of liquid compartments *in vivo*. Conversely, ADP and AMP exhibited comparatively lower efficiency in dissolving protein condensates, suggesting the triphosphate moiety plays a considerable role in protein condensate dissolution. Additionally, only TP-Mg had a negligible effect on protein drop dissolution, indicating that the charge density in the ionic ATP side chain alone is insufficient for dissolving protein drops. Together, these findings highlight the efficiency of ATP as a protein aggregate solubilizer, which stems from its specific chemical structure and not merely its amphiphilicity.

According to the suggestion of the reviewer we have included the discussion in the revised manuscript as "Comparing the effects of ATP with other nucleotides such as ADP and GTP, we emphasize that previous studies have demonstrated GTP can dissolve protein droplets (such as FUS) with efficiency comparable to ATP. However, *in vivo*, the concentration of GTP is significantly lower than that of ATP, resulting in negligible impact on the solubilization of liquid compartments. In contrast, ADP and AMP show much lower efficiency in dissolving protein condensates, indicating the critical role of the triphosphate moiety in protein condensate dissolution. Furthermore, only TP-Mg exhibited a negligible effect on protein droplet dissolution, suggesting that the charge density in the ionic ATP side chain alone is insufficient for this process. These findings underscore ATP's superior efficacy as a protein aggregate solubilizer, attributed to its specific chemical structure rather than merely its amphiphilicity." (page 15).

(iv) In Figure 2F, it seems that in the presence of 0.5 M ATP, the R_g increases (as expected), but the number of native contacts remains almost similar. The reduction in the number of native contacts at higher ATP concentrations is not as dramatic as the increase in R_g . This is somewhat counterintuitive and should be looked into. Normally one would expect a monotonous reduction in the number of native contacts as the protein unfolds (increase in R_g).

We appreciate the reviewer's insightful comment. As noted, the presence of 0.5 M ATP results in an increase in the protein's radius of gyration (R_g) and a decrease in native contacts, indicating that ATP promotes protein chain extension. However, the extent of the changes in R_g and native contacts are not identical. It is important to recognize that even the disruption of a few native contacts can significantly impact protein folding, leading to considerable protein chain extension. Therefore, it is not necessary for the extent of variation in R_g and native contacts to be similar. The appropriate measure is whether the alterations in these two variables are consistent with each other, such that an increase in R_g is accompanied by a decrease in native contacts, and vice versa.

Reviewer #1 (Recommendations For The Authors):

(i) There are several references repeated multiple times, e.g. (a) 1, 9, 14, (b) 25, 29, 31, 33. There are more such examples and the authors should fix these.

We thank the reviewer for pointing this out. We have addressed the issue in the updated manuscript.

(ii) Specific Gromacs version should be mentioned rather than 20xx.

In the updated manuscript we have mentioned the particular version of Gromacs software (2018.6) we have employed for our simulation.

Reviewer #2 (Public Review):

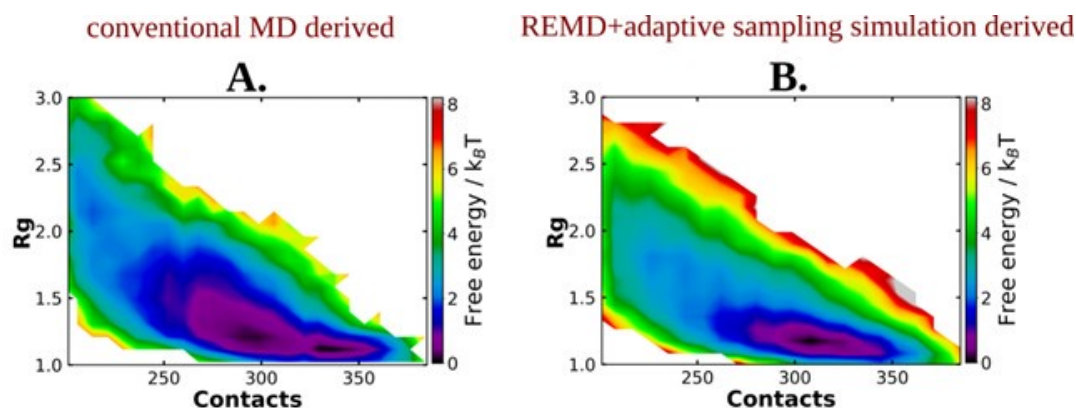
In this work, Sarkar et al. investigated the potential ability of adenosine triphosphate (ATP) as a solubilizer of protein aggregates by combining MD simulations and ThT/TEM experiments. They explored how ATP influences the conformational behaviors of Trp-cage and β -amyloid A β 40 proteins. Currently, there are no experiments in the literature supporting their simulation results of ATP on Trp-cage. The simulation protocol employed for the A β 40 monomer system is conventional MD simulation, while REMD simulation (an enhanced sampling method) is used for the A β monomer + ATP system. It is not clear whether the conformational difference is caused by ATP or by the different simulation methods used.

We thank the reviewer for raising this point. First we note that for Trp-cage, the simulation methods employed in presence and absence of ATP were identical (REMD simulation) and the difference in the free energy surfaces due to introduction of ATP in the solution were evident.

Nonetheless to address referee's point if the difference in simulation method employed for generating the 2D free energy landscape in absence and presence of ATP would have introduced the observed difference, we had undertaken the initiative of carrying out a fresh set of REMD simulations with A β 40 in neat water, followed by adaptive sampling simulation. As shown below in Author response image 1, the free energy profiles obtained from conventional MD simulation (using DESRES trajectory) as well as those obtained via REMD simulations for the same system (in neat water) are qualitatively similar. The free energy profiles obtained in presence of ATP are significantly different from that of neat water, irrespective of the simulation method. This confirms the simulation's observation of ATP driven alteration of protein conformation.

Author response image 1.

Image represents the 2D free energy profile for A β 40 monomer in absence of ATP, obtained through A. conventional MD and B. REMD simulation followed by adaptive sampling simulation.



In the revised manuscript we have included the discussion as “To verify that the effect of ATP on conformational landscape is not an artifact of difference in sampling method (long conventional MD in absence of ATP versus REMD in presence of ATP), we repeated the conformational sampling in absence of ATP via employing REMD, augmented by adaptive sampling (figure S4). We find that the free energy map remains qualitatively similar (figure 4A and S4) irrespective the sampling technique. Comparison of 2D free energy map obtained from REMD simulation in absence of ATP (figure S4) with the one obtained in presence of ATP (figure 4B) also indicates ATP driven protein chain elongation.” on page 7 and updated the method section as “To test the robustness we have also estimated the 2D free energy profile of A β 40 in absence of ATP by performing a similar REMD simulation followed by adaptive sampling simulation following the similar protocol described above.” on page 20.

ThT/TEM experiments should be performed on A β 40 fibrils rather than on A β (16-22) aggregates. Moreover, to elucidate their experimental results that ATP can dissolve preformed A β fibrils, the authors need to study the influence of ATP on A β fibrils instead of on A β dimer in their MD simulations. The novelty of this study is limited. The role of ATP in inhibiting A β fibril formation and dissolving preformed A β fibrils has been reported in previous experimental and computational studies (Journal of Alzheimer's Disease, 2014, 41: 561; Science 2017, 2017, 356, 753-756 J. Phys. Chem. B 2019, 123, 9922–9933; Scientific Reports, 2024, 14: 8134). However, most of those papers are not discussed in this manuscript. Additionally, some details of MD simulations and data analysis are missing in the manuscript, including the initial structures of all the simulations, the method for free energy calculation, the dielectric constant used, etc.

We thank the reviewer for pointing out additional papers on ATP that were not discussed in the original manuscript. While some of the suggested papers were already cited (Science 2017, 356, 753-756), we had initially excluded the others as we did not find them directly relevant to our focus. However, in this revised version, we have included those references (on page 17 and 18).

Through a thorough literature review, including the papers suggested by the reviewer, we maintain that our article is novel in its investigation of ATP's role in the protein conformational landscape and its correlation with anti-aggregation effects. While previous reports emphasize ATP's role in inhibiting protein aggregation, our work connects these findings by highlighting ATP's influence starting at the monomeric level, thereby preventing proteins from becoming aggregation-prone.

In the revised manuscript, we have included this justification as “While previous reports emphasize ATP's role in inhibiting protein aggregation, our work connects these findings by highlighting ATP's influence starting at the monomeric level, thereby preventing proteins from becoming aggregation-prone.” on page 18.

Regarding the reviewer's concern on the details of MD simulations, we would like to mention that method part of the current article provides an elaborate explanation of the simulation set up and characterization (on page 19-21). Regarding the reviewer's comment on dielectric constant, we would like to emphasize that here we have performed simulation considering explicit presence of solvent (water molecules), which by default takes into account dielectric constants (unlike many approximate continuum modelling approaches).

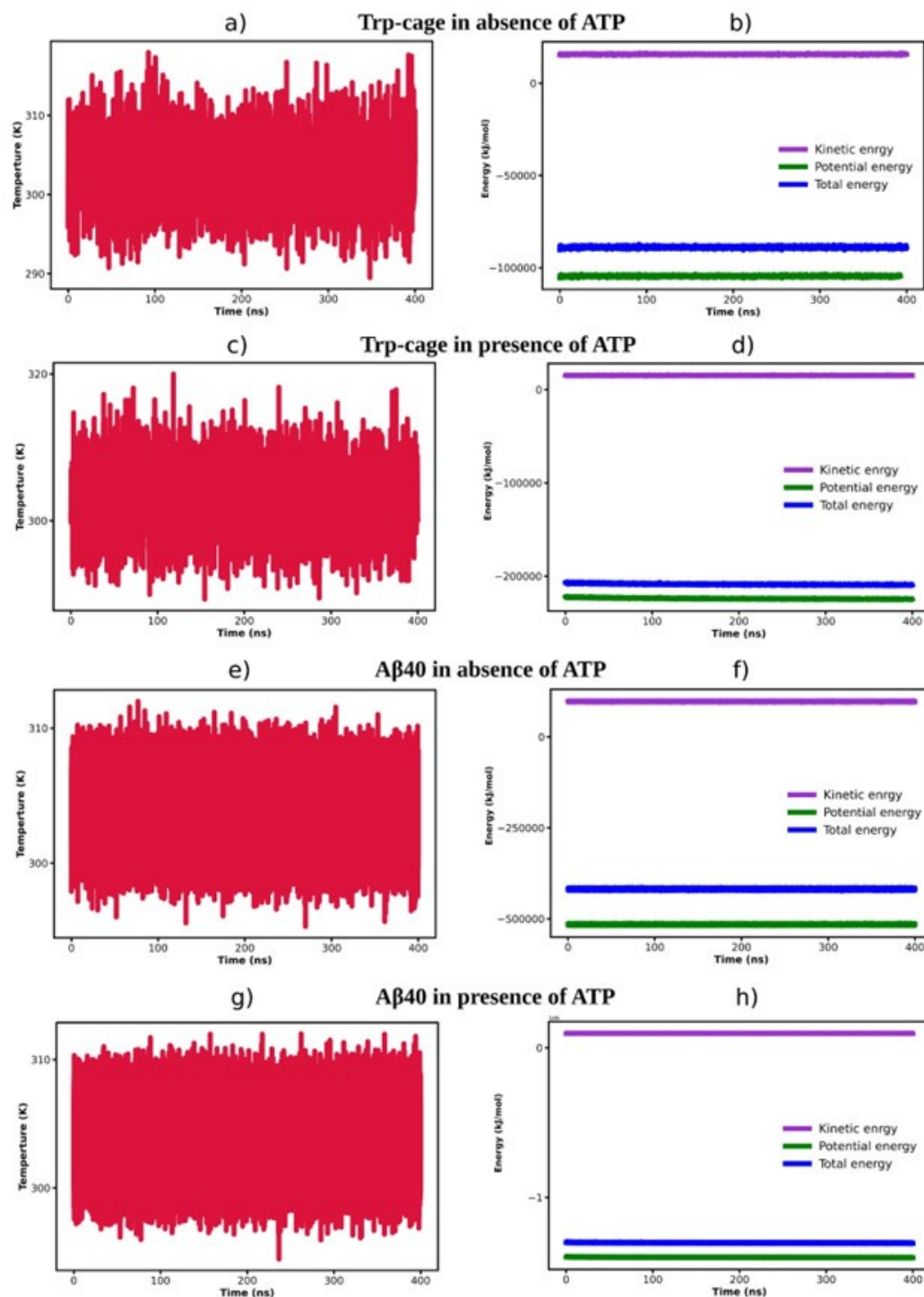
Reviewer #2 (Recommendations For The Authors):

(1) The convergence of simulations needs to be verified prior to data analysis.

We thank the reviewer for this suggestion. We have assessed the convergence of the simulations and represented the respective plots in Author response image 2.

Author response image 2.

The time profile of temperature (a, c, e and g) and energies i.e. kinetic energy, potential energy and total energy (b, d, f and h) are being represented for Trp-cage in absence (a-b) and presence of 0.5 MATP (c-d) and A β 40 protein in absence (e-f) and presence of 0.5 M ATP (g-h).



(2) "The precedent experiments investigating protein aggregation in the presence of ATP, had been performed by maintaining the ATP:protein stoichiometric ratio in the range of 0.1×10^3 to 1.6×10^3 . Likewise, in our simulation with Trp-cage, the ATP:protein ratio of 0.02×10^3 was maintained." Clearly, there is a big difference between the ATP:protein ratio in the MD simulations and that in the precedent experiments.

We thank the reviewer for raising this point. We would like to clarify that for unstructured proteins, including Aβ40, the ATP stoichiometry [1] ranged from 0.1×10^3 to 1.6×10^3 . In our

study, we have maintained the ATP stoichiometry at 0.1×10^3 for the disordered protein A β 40. For structured globular mini-protein like Trp-cage, a lower concentration of 0.02×10^3 was used, consistent with other studies investigating the effects of ATP on globular proteins such as ubiquitin, lysozyme, and malate dehydrogenase, where the ATP stoichiometry ranged [13] from 0.01×10^3 to 0.03×10^3 .

In the revised manuscript we have clearly mentioned the point as “The precedent studies reporting the effect of ATP on structured proteins, had been performed by maintaining ATP:protein stoichiometric ratio in the range of 0.01×10^3 to 0.03×10^3 . Likewise, in our simulation with Trp-cage, the ATP:protein ratio of 0.02×10^3 was maintained.” in page 4 and “The former experiments investigating protein (unstructured) aggregation in presence of ATP, had been performed by maintaining ATP:protein stoichiometric ratio in the range of 0.1×10^3 to 1.6×10^3 , similarly we have also maintained ATP/protein stoichiometry 0.1×10^3 in our investigation ATP’s effect on disordered protein A β 40.” in page 7.

However, during our experimental measurements we have maintained micromolar concentration of protein and ATP concentration in the millimolar range, which lies consistent with the former in vitro experimental studies [1].

(3) The snapshots in Figure 2G show that in the absence of ATP, the Trp-cage monomer exhibits only minor conformational changes compared to the NMR structure (PDB: 1L2Y). However, the native contact number of the Trp-cage monomer (~18, Figure 2C) is much smaller than the total contact number (~160, Figure 2B). The authors are suggested to explain this unexpectedly large difference.

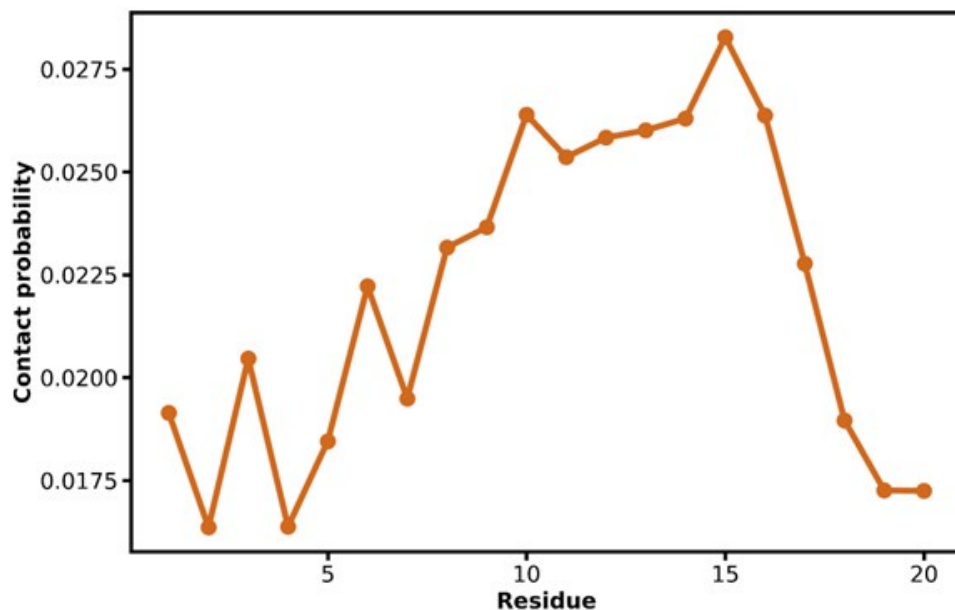
The authors thank the reviewer for his/her concern related to the values of native contact and the total number of contacts of the protein Trp-cage. The author would like to highlight that the estimation of total number of contacts involves the cumulative number of intra-protein contacts which calculates when the two atoms of the protein’s come within the cut-off distance (0.8 nm). Whereas native contact only considers the key contacts of the protein between the side chains of two amino acids that are not adjacent in the amino acid sequence.

(4) The authors are suggested to calculate the contact numbers of each residue with different parts of ATP (phosphate group, base, and sugar moiety), which will help to reveal the key interactions between ATP and proteins.

The authors thank the reviewer for this comment. According to the suggestion we have calculated the contact probability of each residue of protein with ATP as depicted in Author response image 3 and 4 for Trp-cage and A β 40 respectively.

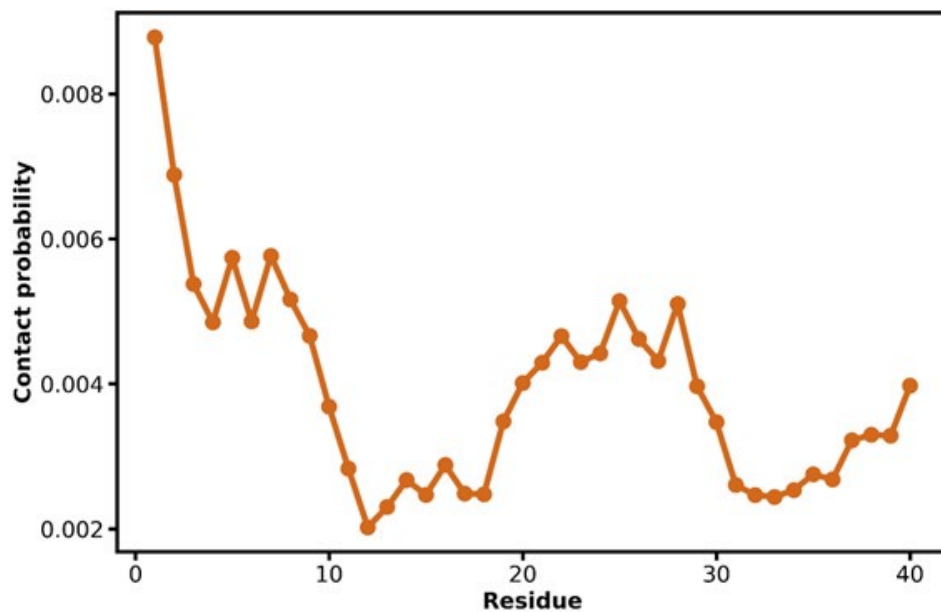
Author response image 3.

The figure shows the residue wise contact probability of protein Trp-cage with ATP.



Author response image 4.

The image shows the residue wise contact probability of A β 40 protein with ATP.



For detailed interaction of ATP's region-specific interactions with proteins, the authors would like to refer to the calculation of the preferential binding coefficient and interaction energies as depicted in Figure 3 for Trp-cage (in page 6) and in Figure 5 and 8 for A β 40 protein. These

figures illustrate well the mode of protein interaction with the chemically divergent regions of ATP and also illuminates ATP's interaction with different parts of the proteins as well.

(5) The authors claimed that "coulombic interaction of ATP with protein predominates in A β 40 (Figure 5 H)" (Page 10). However, the preferential interaction coefficient in Figure 5G shows that the curve of the phosphate group lies below the other two curves when distance < 1 nm, indicating the relatively weak interactions between the phosphate group and A β 40. This seems to be in conflict with the results of energy calculation (Figure 5H).

We thank the reviewer for raising this point. The author would like to emphasize that ATP, with its large and highly charged phosphate group, is highly likely to interact with intrinsically disordered proteins (IDPs) primarily through electrostatic interactions due to their significant charge content. In Figure 5G, it is evident that the preferential binding coefficient reaches a notably high value, indicating strong interaction between the protein and the charged phosphate group of ATP. To address the reviewer's concern regarding the curve showing the highest interaction value only after 1 nm, we would like to highlight the nature of long-range electrostatic potential, which is active in the range of approximately 1–1.2 nm [14–16]. Furthermore, Figure 5H confirms that the electrostatic interaction between the protein and ATP is favorable and predominates over the Lennard-Jones (LJ) interaction.

(6) There are several issues with citations. For example, references 2, 5, 24, 28, 32, 45, 49 and 53 are the same paper, references 1, 7, and 14 are the same paper, references 12, 15, and 46 are the same paper, and many more. In addition, the title of reference 12/15 is "ATP Controls the Aggregation of A β 16-22 Peptides" instead of "ATP Controls the Aggregation of A β Peptides".

We thank the reviewer for pointing this out. We have addressed the issue in the updated manuscript.

(7) References 19 and 20 are cited in the context of "As a potential function of the excess ATP concentration within the cell, a substantial influence on cellular protein homeostasis is observed, particularly in preventing protein aggregation (14-21)" (Page 2). However, there is no mention of "ATP" in ref. 19 and 20.

Thank you to the reviewer for identifying this mistake. We have corrected the issue in the revised manuscript.

(8) On page 22: "To perform all the molecular dynamics (MD) simulations GROMACS software of version 20xx software was utilized". Please provide the version of GROMACS software used in this study.

In the updated manuscript, we have specified the particular version of Gromacs software (2018.6) used for our simulations. (see revised manuscript page 19)

(9) In Figure 8J, the time-dependent distance of A β 40 dimer without ATP needs to be provided as a comparison.

We thank the reviewer for this comment. In the revised manuscript we have updated the calculation of distance between the A β 40 protein chains both in absence and presence of ATP as well as "The probability distribution (Figure 8J) illustrates that, in the presence of ATP, the two protein chains, initially part of the dimer, become prone to be moved away from each other." (page 15).

(10) *The authors should compare ATP-A β interactions with NaXS-A β interactions to understand why ATP is more efficient than NaXS in inhibiting interprotein interactions.*

The authors thank the reviewer for the concern regarding the ATP-A β 40 interaction compared to the NaXS-A β 40 interaction. We would like to highlight our results (Figure 5G and H) which demonstrate the dominance of Coulombic interactions (over LJ interactions) of ATP with the protein. Based on this, we compared the Coulombic interaction energy of ATP and NaXS with the protein A β 40, as depicted in Figure 9I. We observed that ATP-protein electrostatic interactions occur more favorably than those with NaXS, leading to better action of ATP over NaXS. The favorable electrostatic interaction of ATP with the protein, compared to NaXS, is evident because ATP possesses a large and highly charged triphosphate group that can strongly interact with the protein, whereas NaXS contains a very small sulfonate group with much less charge. Therefore, due to the favorable Coulombic interaction of ATP with the protein over NaXS, ATP acts more efficiently as a hydrotrope. In the revised manuscript we have highlighted the term “Coulombic interaction” in the main text and in the figure caption (Figure 9) as well (in page 15 and 16 of the revised manuscript respectively).

(11) *The word "solubilizer" in the Abstract is a typo.*

We thank the reviewer for pointing this out. We have made the necessary corrections in the revised manuscript.

(12) *What does "ATP-Mg²⁺" mean in the manuscript?*

ATP, being polyanionic and possessing a potentially chelating polyphosphate group, binds metal cations with high affinity and hence biologically it occurs to be complexed with the equivalent number of Mg²⁺ in the form of ATP-Mg [17–19]. Similarly multiple former studies utilized ATP-Mg in their investigations [1,20–22].

Reviewer #3 (Public Review):

Summary:

Since its first experimental report in 2017 (Patel et al. Science 2017), there have been several studies on the phenomenon in which ATP functions as a biological hydrotrope of protein aggregates. In this manuscript, by conducting molecular dynamics simulations of three different proteins, Trp-cage, Abeta40 monomer, and Abeta40 dimer at a high concentration of ATP (0.1, 0.5 M), Sarkar et al. find that the amphiphilic nature of ATP, arising from its molecular structure consisting of phosphate group (PG), sugar ring, and aromatic base, enables it to interact with proteins in a protein-specific manner and prevents their aggregation and solubilize if they aggregate. The authors also point out that in comparison with NaXS, which is the traditional chemical hydrotrope, ATP is more efficient in solubilizing protein aggregates because of its amphiphilic nature.

Trp-cage, featured with a hydrophobic core in its native state, is denatured at high ATP concentration. The authors show that the aromatic base group (purine group) of ATP is responsible for inducing the denaturation of helical motifs in the native state.

For Abeta40, which can be classified as an IDP with charged residues, it is shown that ATP disrupts the salt bridge (D23-K28) required for the stability of beta-turn formation.

By showing that ATP can disassemble preformed protein oligomers (Abeta40 dimer), the authors argue that ATP is "potent enough to disassemble existing protein droplets, maintaining proper cellular homeostasis," and enhancing solubility.

Overall, the message of the paper is clear and straightforward to follow. I did not follow all the literature, but I see in the literature search, that there are several studies on this subject. (J. Am. Chem. Soc. 2021, 143, 31, 11982-11993; J. Phys. Chem. B 2022, 126, 42, 8486-8494; J. Phys. Chem. B 2021, 125, 28, 7717-7731; J. Phys. Chem. B 2020, 124, 1, 210-223).

If this study is indeed the first one to test using MD simulations whether ATP is a solubilizer of protein aggregates, it may deserve some attention from the community. But, the authors should definitely discuss the content of existing studies, and make it explicit what is new in this study.

Strengths:

The authors showed that due to its amphiphilic nature, ATP can interact with different proteins in a protein-specific manner, a finding more general and specific than merely calling ATP a biological hydrotrope.

Weaknesses:

(1) My only major concern is that the simulations were performed at unusually high ATP concentrations (100 and 500 mM of ATP), whereas the real cellular concentration of ATP is 1-5 mM. Even if ATP is a good solubilizer of protein aggregates, the actual concentration should matter. I was wondering if there is a previous report on a titration curve of protein aggregates against ATP, and what is the transition mid-point of ATP-induced solubility of protein aggregates.

For instance, urea or GdmCl have long been known as the non-specific denaturants of proteins, and it has been well experimented that their transition mid-point of protein unfolding is $\sim(1 - 6)$ M depending on the proteins.

We thank the reviewer for their concern regarding the ATP concentration used in our simulation. The reviewer correctly noted our statement about cellular ATP concentrations being in the range of a few millimolar. We would like to highlight that, in a cellular environment, millimolar ATP concentrations coexist with micromolar protein concentrations in the aqueous phase.

In our study, we focused on the impact of ATP on protein conformational dynamics, primarily simulating a protein monomer within the simulation box. To maintain a micromolar protein concentration (e.g., 20 μ M [1]) for a monomeric protein, a simulation box of significant dimensions ($\sim 44 \times 44 \times 44$ nm³) would be required. This size would be computationally challenging to simulate at an atomistic resolution due to the excessive computational cost and time.

To ensure computational efficiency, we employed millimolar protein concentrations instead of micromolar, thus requiring a higher ATP concentration to maintain the cellular protein stoichiometry. Similar to the stoichiometry in the cellular environment (i.e., micromolar protein : millimolar ATP ~ 103), our simulations maintained a consistent ratio (i.e., millimolar protein : molar ATP ~ 103). This approach allowed us to use a smaller simulation box while preserving the relevant stoichiometry, enabling us to leverage data within a realistic timeframe.

Based on the reviewer comment we have included the explanation in the revised manuscript as "In this study, we opted to maintain the ATP stoichiometry consistent with biological conditions and previous in vitro experiments. Instead of keeping the protein concentration within the micromolar range and ATP concentration at the millimolar level, we chose this

approach to avoid the need for an extremely large simulation box, which would greatly reduce computational efficiency by more than 150-fold.” (page 4).

However, during our experimental measurements we have maintained micromolar concentration of protein and ATP concentration in the millimolar range, which lies consistent with the former in vitro experimental studies [1]

(2) The sentence "... a clear shift of relative population of Abeta40 conformational subensemble towards a basin with higher Rg and lower number of contacts in the presence of ATP" is not a precise description of Figures 4A and 4B. It is not clear from the figures whether the Rg of Abeta40 is increased when Abeta40 is subject to ATP. The authors should give a more precise description of what is observed in the result from their simulations or consider a better-order parameter to describe the change in molecular structure.

We thank the reviewer for this comment. Figure 4A and 4B depicting the 2D free energy profile of the Aβ40 protein with respect to Rg and total number contacts are presented to pinpoint the alteration of protein conformational landscape in influence of ATP. To further elucidate ATP driven protein conformational alteration, the overlaid snapshots corresponding to absence and presence of ATP were also provided. Together the author believes that the descriptions of Figures 4A and 4B in the article are appropriate and effectively incorporate the analysis provided in the article.

In addition, the disruption of beta-sheet from Figure 4E to 4F is not very clear. The authors may want to use an arrow to indicate the region of the contact map associated with this change.

In the revised manuscript the authors have highlighted the region of the contact map associated with the changes in the beta-sheet propensity with an arrow for each of the plots.

Although the full atomistic simulations were carried out, the analyses demonstrated in this study are a bit rudimentary and coarse-grained (e.g, Rg is a rather poor order parameter to discuss dynamics involved in proteins). The authors could go beyond and say more about how ATP interacts with proteins and disrupts the stable configurations.

We thank the reviewer for this comment. We understand the reviewer's concern regarding the choice of the order parameter (Rg), which has been a topic of long-standing debate. However, we would like to note that in the current study, we employed Rg based on recent investigations by Dr. D. E. Shaw Research group [23] (specifically concerning the protein Aβ40 and the Charmm36m force field), which reported an almost negligible Rg penalty compared to experimental values. The experiments characterizing IDPs utilize Rg as a choice of metric. We also would like to highlight that previous investigations of our group have done careful benchmarking of several features of proteins as well as IDPs using both linear and artificial neural network based dimension reduction techniques and have demonstrated that Rg, in combination with fraction of native contact serves as optimum features [24,25]. Therefore, we believed that Rg would be a suitable order parameter for analyzing the structural behavior of this protein. Additionally, we have also analyzed other relevant characteristics, including the total number of contacts, residue-wise protein contact map, percentage of secondary structure, solvent-accessible surface area, and distances between key interacting residues, to provide a comprehensive understanding.

The justification of our choice of collective variable has been discussed in the revised manuscript as “Since multiple previous studies has reported benchmarking of several features of proteins as well as IDPs using both linear and artificial neural network based dimension reduction techniques and have demonstrated that Rg, in combination with

fraction of native contact serves as optimum features, we have chosen these two metrics for developing the 2D free energy profile.” on page 4.

(3) Although the amphiphilic character of ATP is highlighted, a similar comment can be made as to GTP. Is GTP, whose cellular concentration is ~0.5 mM, also a good solubilizer of protein aggregates? If not, why? Please comment.

In response to the reviewer’s comment on comparing ATP’s effect with other nucleotides GTP, we would like to highlight that previous studies have shown GTP’s ability to dissolve protein droplets (FUS) with similar efficiency to ATP [1,26]. However, in cells, the concentration of GTP is much lower than that of ATP, resulting in negligible effects on the solubilization of liquid compartments in vivo [1].

According to the suggestion of the reviewer we have included the discussion in the revised manuscript as “Comparing the effects of ATP with other nucleotides such as ADP and GTP, we emphasize that previous studies have demonstrated GTP can dissolve protein droplets (such as FUS) with efficiency comparable to ATP. However, in vivo, the concentration of GTP is significantly lower than that of ATP, resulting in negligible impact on the solubilization of liquid compartments. In contrast, ADP and AMP show much lower efficiency in dissolving protein condensates, indicating the critical role of the triphosphate moiety in protein condensate dissolution. Furthermore, only TP-Mg exhibited a negligible effect on protein droplet dissolution, suggesting that the charge density in the ionic ATP side chain alone is insufficient for this process. These findings underscore ATP’s superior efficacy as a protein aggregate solubilizer, attributed to its specific chemical structure rather than merely its amphiphilicity.” (page 15).

Reviewer #3 (Recommendations For The Authors):

Spell-check should be carried out throughout the manuscript. e.g., sollubilizer, sollubilizing, ...

We thank the reviewer for pointing this out. We have made the necessary corrections in the revised manuscript.

The reference section should be properly organized. There are multiple repetitions of references (e.g., references 28, 30, 32 are the same reference). I see many instances of this.

We thank the reviewer for pointing this out. We have addressed the issue in the updated manuscript.

References:

- (1) Patel, A.; Malinowska, L.; Saha, S.; Wang, J.; Alberti, S.; Krishnan, Y.; Hyman, A. A. ATP as a Biological Hydrotrope. *Science* 2017, 356 (6339), 753–756.
- (2) Ren, C.-L.; Shan, Y.; Zhang, P.; Ding, H.-M.; Ma, Y.-Q. Uncovering the Molecular Mechanism for Dual Effect of ATP on Phase Separation in FUS Solution. *Sci Adv* 2022, 8 (37), eabo7885.
- (3) Song, J. Adenosine Triphosphate Energy-Independently Controls Protein Homeostasis with Unique Structure and Diverse Mechanisms. *Protein Sci.* 2021, 30 (7), 1277–1293.
- (4) Liu, F.; Wang, J. ATP Acts as a Hydrotrope to Regulate the Phase Separation of NBDY Clusters. *JACS Au* 2023, 3 (9), 2578–2585.
- (5) Chu, X.-Y.; Xu, Y.-Y.; Tong, X.-Y.; Wang, G.; Zhang, H.-Y. The Legend of ATP: From Origin of Life to Precision Medicine. *Metabolites* 2022, 12 (5). <https://doi.org/10.3390/metabo12050461>.

- (6) Tian, Z.; Qian, F. Adenosine Triphosphate-Induced Rapid Liquid-Liquid Phase Separation of a Model IgG1 mAb. *Mol. Pharm.* 2021, 18 (1), 267–274.
- (7) Wang, B.; Zhang, L.; Dai, T.; Qin, Z.; Lu, H.; Zhang, L.; Zhou, F. Liquid-Liquid Phase Separation in Human Health and Diseases. *Signal Transduct Target Ther* 2021, 6 (1), 290.
- (8) Alberti, S.; Dormann, D. Liquid-Liquid Phase Separation in Disease. *Annu. Rev. Genet.* 2019, 53, 171–194.
- (9) Nair, K. S. Aging Muscle. *Am. J. Clin. Nutr.* 2005, 81 (5), 953–963.
- (10) Recharging Mitochondrial Batteries in Old Eyes. Near Infra-Red Increases ATP. *Exp. Eye Res.* 2014, 122, 50–53.
- (11) Goldberg, J.; Currais, A.; Prior, M.; Fischer, W.; Chiruta, C.; Ratliff, E.; Daugherty, D.; Dargusch, R.; Finley, K.; Esparza-Moltó, P. B.; Cuezva, J. M.; Maher, P.; Petrascheck, M.; Schubert, D. The Mitochondrial ATP Synthase Is a Shared Drug Target for Aging and Dementia. *Aging Cell* 2018, 17 (2). <https://doi.org/10.1111/acer.12715>.
- (12) Kagawa, Y.; Hamamoto, T.; Endo, H.; Ichida, M.; Shibui, H.; Hayakawa, M. Genes of Human ATP Synthase: Their Roles in Physiology and Aging. *Biosci. Rep.* 1997, 17 (2), 115–146.
- (13) Ou, X.; Lao, Y.; Xu, J.; Wutthinitikornkit, Y.; Shi, R.; Chen, X.; Li, J. ATP Can Efficiently Stabilize Protein through a Unique Mechanism. *JACS Au* 2021, 1 (10), 1766–1777.
- (14) Norberg, J.; Nilsson, L. On the Truncation of Long-Range Electrostatic Interactions in DNA. *Biophys. J.* 2000, 79 (3), 1537–1553.
- (15) Pabbathi, A.; Coleman, L.; Godar, S.; Paul, A.; Garlapati, A.; Spencer, M.; Eller, J.; Alper, J. D. Long-Range Electrostatic Interactions Significantly Modulate the Affinity of Dynein for Microtubules. *Biophys. J.* 2022, 121 (9), 1715–1726.
- (16) Sastry, M. Nanoparticle Thin Films: An Approach Based on Self-Assembly. In *Handbook of Surfaces and Interfaces of Materials*; Elsevier, 2001; pp 87–123.
- (17) Wilson, J. E.; Chin, A. Chelation of Divalent Cations by ATP, Studied by Titration Calorimetry. *Anal. Biochem.* 1991, 193 (1), 16–19.
- (18) Storer, A. C.; Cornish-Bowden, A. Concentration of MgATP²⁻ and Other Ions in Solution. Calculation of the True Concentrations of Species Present in Mixtures of Associating Ions. *Biochem. J* 1976, 159 (1), 1–5.
- (19) Garfinkel, L.; Altschuld, R. A.; Garfinkel, D. Magnesium in Cardiac Energy Metabolism. *J. Mol. Cell. Cardiol.* 1986, 18 (10), 1003–1013.
- (20) Hautke, A.; Ebbinghaus, S. The Emerging Role of ATP as a Cosolute for Biomolecular Processes. *Biol. Chem.* 2023, 404 (10), 897–908.
- (21) Pal, S.; Roy, R.; Paul, S. Deciphering the Role of ATP on PHF6 Aggregation. *J. Phys. Chem. B* 2022, 126 (26), 4761–4775.
- (22) Pal, S.; Paul, S. ATP Controls the Aggregation of A β Peptides. *J. Phys. Chem. B* 2020, 124(1), 210–223.
- (23) Robustelli, P.; Piana, S.; Shaw, D. E. Developing a Molecular Dynamics Force Field for Both Folded and Disordered Protein States. *Proc. Natl. Acad. Sci. U. S. A.* 2018, 115 (21), E4758–E4766.

(24) Ahalawat, N.; Mondal, J. Assessment and Optimization of Collective Variables for Protein Conformational Landscape: GB1 -Hairpin as a Case Study. *J. Chem. Phys.* 2018, 149 (9), 094101.

(25) Menon, S.; Adhikari, S.; Mondal, J. An Integrated Machine Learning Approach Delineates Entropy-Mediated Conformational Modulation of α -Synuclein by Small Molecule, 2024. <https://doi.org/10.7554/eLife.97709.1>.

(26) Pandey, M. P.; Sasidharan, S.; Raghunathan, V. A.; Khandelia, H. Molecular Mechanism of Hydrotropic Properties of GTP and ATP. *J. Phys. Chem. B* 2022, 126 (42), 8486–8494.

<https://doi.org/10.7554/eLife.99150.2.sa0>